CHALMERS


# Modeling the Interaction between Intracranial Pressure and Cerebral Hemodynamics

**Master's Thesis in Biomedical Engineering**

Zhaleh Pirzadeh

**Department of Signals and Systems**

**Division of Signal Processing and Antennas**

**CHALMERS UNIVERSITY OF TECHNOLOGY**

**Göteborg, Sweden 2009**

**Report No. Ex083/2009**

REPORT NO. Ex083/2009

# Modeling the Interaction between Intracranial Pressure and Cerebral Hemodynamics

Zhaleh Pirzadeh

Department of Signals and Systems
CHALMERS UNIVERSITY OF TECHNOLOGY

Göteborg, Sweden 2009

Modeling the Interaction between Intracranial Pressure and Cerebral Hemodynamics

Zhaleh Pirzadeh



Technical report no Ex083/2009
Department of Signals and Systems
Chalmers University of Technology
SE-412 96 Göteborg
Sweden
Telephone +46-(0)31 772 10 00

Chalmers Reproservice
Göteborg, Sweden 2009

## Abstract

Uncontrolled increase in ICP is one of the main causes for mortality of patients with traumatic brain injury (TBI) due to secondary brain injury. On the other hand since ICP is not merely affected by hypertension/hypotension but also cerebral hemodynamics, studying ICP time pattern might lead to a good knowledge of patients' cerebral hemodynamics, cerebral perfusion and autoregulation reserve. Thus sufficient quantitative knowledge of ICP monitoring and its dynamics have been recently proved to be of a great clinical importance. Accordingly finding non-invasive approaches in order to measure and monitor ICP and simulate dynamics of human brain has recently become a center of attention for some researchers in the relevant area.

The invasive methods have been introduced and utilized for last decades but it has been proved than this method is not adequate in providing all important information about status of human brain. Thus there is a crucial need for improved methods that can provide specialists with more information about intracranial pressure, cerebral hemodynamics and the relationship between them for a better understanding of patients' brain state.

During this study, after an extensive review over existing suggested approaches a simple mathematical model has been chosen. A qualitative description of the model compartments and relevant equations are presented. An analytical study of ICP instability and generation of plateau waves is performed in order to specify which features variation lead to formation of self sustained unstable ICP oscillation (bifurcation diagram). Another analytical study was carried out to find and estimate parameter values to which ICP shows its most significant sensitivity. The results indicate that although the model contains several parameters, only four of them (elasticity coefficient, CSF outflow resistance, autoregulation gain and autoregulation time constant) seem to influence ICP most. The effect of each parameter on ICP and correlation among these parameters provide us valuable information about patient's status. This knowledge could be useful to help neuro-intensive care unit experts in choosing the right treatment based on understanding which changes have the most important effect on ICP and thus are dangerous or beneficial for patient's condition.



**Keywords**: Arterial Blood Pressure; Cerebral Autoregulation; Cerebral Blood Flow; Cerebral Compliance; Cerebrospinal Fluid; Cerebral Hemodynamics; Intracranial Compliance; Intracranial Pressure; Plateau waves; Pressure-volume Index; Traumatic Brain Injury.

# Acknowledgments

Hereby I would like to show my honest and deep appreciation to my supervisor Tomas Mc Kelvey, without whom accomplishment of this thesis would not have been possible. Thank you for your continuous guidance, patience and support. I have learned a lot from our interesting discussions and look forward to assist from them in the research area.

I owe my deepest gratitude to my family. Thank you dad for believing in me and always supporting me in my decisions and life. Thank you for being my friend. Thank you mom for your endless kindness, your love and great sense of understanding. Thank you Panti, Nima and Laleh. Without you I could have never been where I am today. Thanks for supporting me and always being there for me all way long.

Thank you Sima for your time and effort. Last but not least I would like to thank my friends Pär, Yazdan, Jonas and Ehsan for always encouraging me to move on even when it seemed to be impossible.

Thank you,

Zhaleh Pirzadeh

## Table of Contents

## Table of figures

## Table of abbreviations

| | |
|---|---|
| ABP | Arterial Blood Pressure |
| C | Compliance |
| CBF | Cerebral Blood Flow |
| CPP | Cerebral Perfusion Pressure |
| CSF | Cerebrospinal Fluid |
| CVR | Cerebrovascular Resistance |
| G | Gain |
| ICP | Intracranial Pressure |
| P | Pressure |
| q | Flow |
| PVI | Pressure Volume Index |
| R | Resistance |
| TBI | Traumatic Brain Injury |
| V | Volume |

# Chapter 1

## 1. Introduction

Today, condition monitoring, simulation and time domain analysis of human brain dynamics and non-invasive techniques for intracranial pressure measurement have become the center of attention for researchers especially in those cases of dealing with patients suffering from TBI.

The most common method that has been used in order to measure intracranial pressure in patients with severe brain damage is the invasive measurement method based on inserting a catheter into the cranial cavity through a small hole made in the skull for this reason. Recently it has been proved that there are different factors affecting ICP which are not completely taken into consideration while studying different patients' intracranial pressure. Thus introducing new techniques/models that put more effort on understanding different factors influencing ICP is crucial.

The idea behind this thesis is to investigate new mathematical approaches in order to understand some important factors influencing ICP that have been mostly neglected so far. This research can also be used in analyzing intracranial pressure stability and generation of plateau waves, simulating ICP, better understanding of level of hypertension, estimation of most important parameters effecting ICP morphology and studying the correlation among estimation parameters. The main effort is put on improving physiological knowledge of human brain and decreasing the risk of insufficient utilization of introduced models in real clinical approaches due to their complexity.

### 1.1 Background

Intracranial hypertension is caused by raised intracranial pressure (ICP), which is the pressure that can be measured within the cranial cavity between the outer membrane (dura) and the brain tissue including the ventricles within the brain and the spinal compartments. These ventricles and interconnecting passages contain a lubricating or damping fluid known as the cerebrospinal fluid (CSF). The CSF circulates over the surface of the brain, the brain stem and the spinal cord at a rate of about 500 ml/day and has a rate of formation of about 0.4 ml/min. This means that the CSF is renewed 4-5 times every day. Normal ICP is about 10 mm Hg average with dynamic components due to blood pressure and respiration at the same frequencies as heartbeat and respiration, respectively. Raised ICP caused by a pathological condition, when the balance of production and absorption of CSF has broken down, can go up to 70 mm Hg or even higher.

Raised ICP can lead to death and therefore monitoring and patient management is very important for any pathological condition leading to intracranial hypertension. Monitoring changes to ICP is particularly important and the anticipation of changes very helpful to clinicians and nursing staff involved in patient management [1, 2].

Different researches have recently suggested that mathematical models can be useful in order to improve the understanding of ICP pattern and the quantities affecting this pattern in various pathological conditions. Some of these studies concentrated more on specific intracranial dynamics such as intracranial elasticity [3] or cerebrospinal fluid (CSF) production and re-absorption [4, 5] and some included the relationships between these features and intracranial pressure as multicompartmental models [6, 7, 8].

Although these studies have provided the real physiological basis for ICP modeling and simulations, due to their mathematical complexity of relationships and existence of nonlinear equations, they cannot be used in a practical clinical approach. Thus providing a simple mathematical model that can be actually used in diagnosis and clinical experiments is of high value. As usual there is always a tradeoff between simplicity of a model and its accuracy in representing all clinical or physiological related details. Thus a deep understanding of a model's ability and limitations is needed in order to prevent inappropriate expectation of the model.

## 1.2 Purpose

As mentioned, monitoring and control of the ICP is one of the main keys in preventing secondary brain injury due to brain swelling (hypertension). It has been suggested recently that the level of ICP is not only affected by the level of hypertension but also by cerebral hemodynamics. Thus existence of improved models that include the cerebral hemodynamics effect in order to have more accurate estimations of level of hypertension is of great importance.

This thesis work focuses on introducing and the investigation of an improved mathematical model in simulation of intracranial pressure time pattern, estimation of level of hypertension and providing more information about patients' brain state by studying the interaction between the intracranial pressure and cerebral hemodynamics

## 1.3 Methodology

As shown in the block diagram presented in Figure 1.1, this project is first divided into four different phases. The first phase involves and extensive literature study on different existing approaches suggested by researchers for simulating and modeling intracranial pressure and cerebral hemodynamics. Besides being useful for increasing the basic knowledge about modeling and simulation of ICP, this study was helpful for a better comprehension of intracranial pressure, how it is changed during different procedures and what the reasons behind each ICP alterations are.

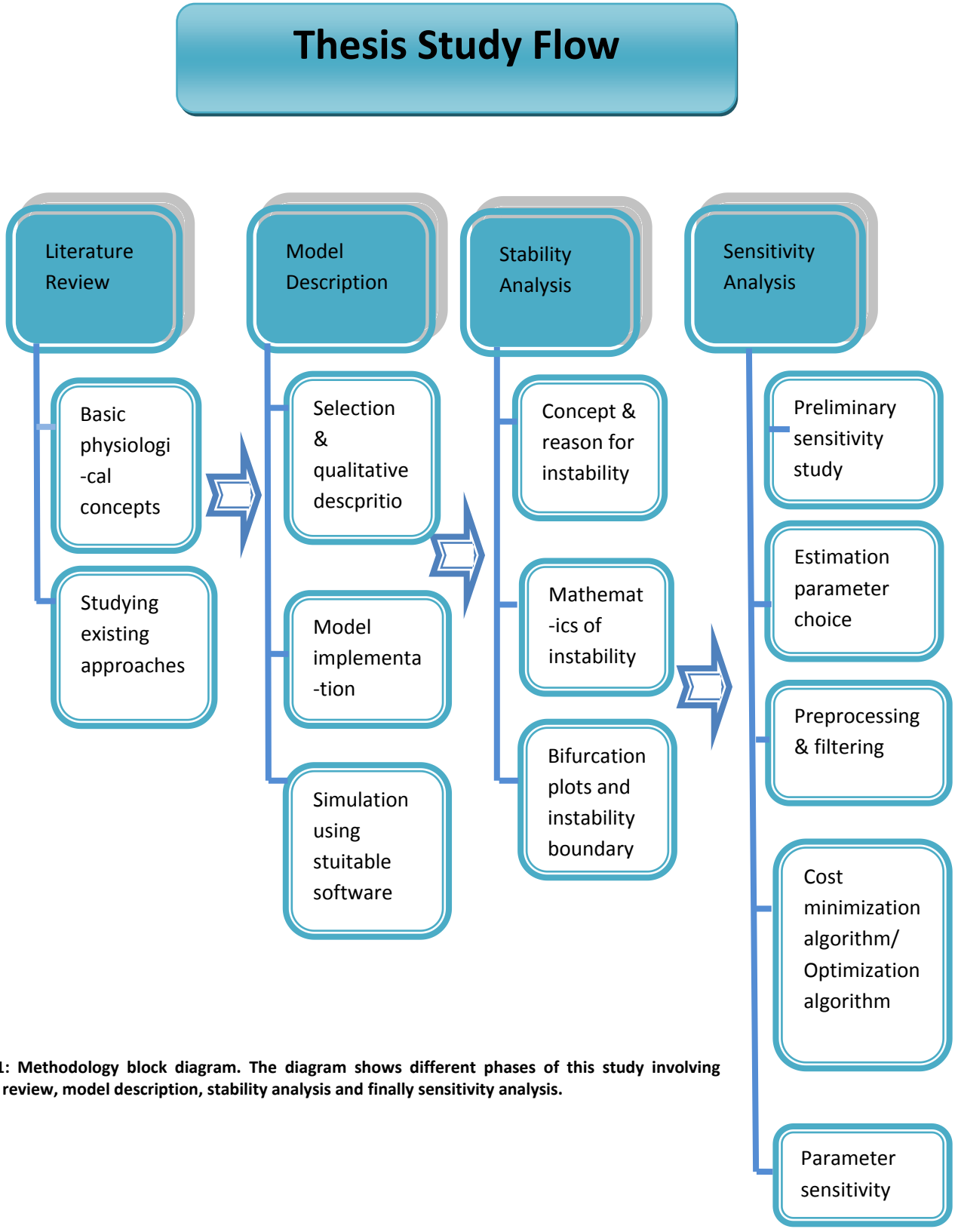


**Figure 1.1: Methodology block diagram. The diagram shows different phases of this study involving literature review, model description, stability analysis and finally sensitivity analysis.**

Second phase involves the selection of suitable model among the relevant suggested ones. The selection was mostly based on the ability of the model in reproducing ICP wave originating from heart pulsations (ABP) and its simplicity and usability in real clinical approaches rather than its being very accurate in tracing all details. After that the model was implemented and simulated via suitable simulation software such as Matlab, Simulink and PLECS.

Third phase includes the stability analysis of the suggested model. As it will be explained in the stability analysis section, since the model has positive feedback there is always a risk of instability. The main goal of the stability analysis was to find out which clinical circumstances lead the model to exhibit instability. Prediction of a boundary between stable and unstable region was done by means of studying specific parameter variations. In other words the variation of those parameters to a specific limit leads to unstable model behavior such as production of plateau waves (A- waves) or self sustained oscillations. This study aimed to find those parameters and their effect on unstable behavior of the model. For this aim first the equations were rewritten in order to gain a general form and then the equilibrium point was calculated for these equations by having constant input and a given set of parameters. After linearization of the equations around the equilibrium point, Jacobian matrix of the system and eigenvalues were computed. Then the parameter values that meet the condition of boundary were saved and plotted to separate the two stable and unstable regions. The results for this stability study are explained more in details in the relevant chapter.

A small part of the fourth phase of the project is devoted to evaluating the model's ability in simulating a valid ICP form for a given patient with a defined arterial blood pressure (ABP) as an input; a preliminary comparison study was done for different patients with different ABP and ICP morphology according to their autoregulatory situations. The model seemed to efficiently simulate and trace the real ICP which was provided by experimental data from Sahlgrenska University Hospital.

The next part of the fourth phase of the project was devoted to a sensitivity analysis of the model. The main goal of the sensitivity analysis was to understand which parameters are needed to be estimated from clinical data and which are needed to be chosen as a priori. First a set of parameters were chosen to be estimated during minimization algorithm. The choice was mostly based on a preliminary study performed to find out which parameters alteration show more impact on ICP time pattern. Using an automatic minimization algorithm, those set of parameters were estimated in a way to minimize the difference between models prediction and experimental recorded ICP. This can be used for automatic parameter tuning with the aim of cost function minimization. On the other hand the sensitivity analysis can be used to yield a better understanding of which parameters have the most significant impact on intracranial pressure time pattern and how their variation affect ICP wave form. During the sensitivity analysis the model was mainly fed with experimental collected patients ABP and ICP as inputs and the model was

examined in producing the ICP that seems to be the best fit with the ICP provided from hospital. The mathematics behind the sensitivity study and some basic knowledge of optimization algorithm are more discussed in the relevant chapter. Then the results of preprocessing, comparison between simulated ICP versus the recorded one, cost function variation and parameter sensitivity plots are presented, explained and analyzed in the results of sensitivity analysis chapter.

# Chapter 2

## 2. Literature review

*In this chapter a brief overview of intracranial pressure measurement history and previous studies performed in the relevant area is presented and for the purpose of better understanding of specific terms used in this research area some of the most common physiological concepts are briefly discussed.*

### 2.1 Literature review

The existence of relationship among intracranial pressure (ICP), cerebral blood volume (CBV) and cerebral hemodynamics and a mathematical explanation of these interrelationships have become the center of attention of some authors during last decades. Several mathematical models have been proposed that each might introduce an almost new feature or procedure in analyzing these relationships.

The history of intracranial hypertension investigation and craniospinal volume-pressure relationships was initiated back in 1783 by Monro and further developed by Kellie afterwards in 1824. Monro introduced a number of valuable observations in his book entitled 'Observations on the structure and function of the nervous system" [9].The original Monro-Kellie doctrine or hypothesis proposed a rigid and extensible cranial cavity, filled to capacity with incompressible brain tissue and blood, from which it was concluded that the volume of the latter must at all times be constant. The doctrine was extremely simple and did not take into account the CSF nor the spinal portion of the craniospinal compartment. This original Monro-Kellie paradigm was gradually modified by various researchers including Burrows in 1846 [10], who postulated that the volume of blood could vary reciprocally with the volume of CSF, and Weed and McKibben in 1919 [11], who showed that with intravenous injections of hypo- and hypertonic solutions the volume of the brain bulk could also be markedly altered. This simple hypothesis did not explain many significant aspects of intracranial dynamics such as the observed effects on ICP of slowly expanding a balloon inside the intracranial vault. Experiments on animals by H. Cushing have shown that the ICP rises slowly at first and more rapidly as the volume increases [12]. This is explained by the initial changes in volume being accommodated by some change or movement of the intracranial content (probably CSF) and the final effects by exhaustion of the cranial content accommodation and the much increased compressibility of the intracranial contents or the craniospinal covering. Ayala discovered that there existed a relationship between pressure and volume by removing CSF and measuring the ensuing pressure changes [13]. This relationship, known as Ayala's index, is defined as change in pressure divided by change in

volume and indicates a type of pathological condition. It has been found to be high with cerebral tumors and low for intracranial hypertension.

Weed and Flexner were the first to investigate systematically the changes in total intracranial volume and changes in ICP and concluded that this complex relationship was neither the rigid model nor the pure elastic model. The relationship was perceived to be a function of the collapsibility and distensibility of the dural sac and intradural and extradural vascular factors [14].

In 1902 Cushing carried out a number of experiments on animals to investigate the effects of local compression as might be caused by tumors and blood clots and general compression caused by hydrocephalus meningitis and subdural hemorrhages [15]. The experiments he conducted used balloons inserted into the intracranial space to produce local compression and fluids (salt solution) connected to the cerebral spinal space to produce general compression. Measurements were taken showing that as ICP rises, blood pressure (BP) rises up to a certain level before death ensues, confirming that a mechanism exists that stimulates the vaso-motor centre to compensate and increase blood pressure and hence blood flow. Ryder et al. [16] developed the modern concepts of pressure volume relationships and in 1971 Shulman and Marmarou [17] published a detailed mathematical model which used the collapsibility of the nervous system and not the elasticity of the dural sac as the physiological basis. CSF pulse wave analysis was used by Foltz and Aine in 1980 for the diagnosis of hydrocephalus [18]. They showed that the 'pulsatility' of the CSF was augmented in hydrocephalus and argued that this 'pulsatility', including the CSF waveform, may be a more valid criterion for the diagnosis of hydrocephalus than mean CSF pressure. To test this possibility, they measured CSF pressures in 118 patients with presumed hydrocephalus, recorded baseline mean pressure and pulse pressure responses to jugular compression, and performed CSF wave analysis (amplitude and peak latency). Four groups of pressure recordings were identified and matched with four clinical groups: normal, arrested hydrocephalus, communicating hydrocephalus, and aqueduct stenosis hydrocephalus. They found that CSF pulse pressure and systolic slope form were highly reliable in the diagnosis of hydrocephalus, whereas mean CSF pressure was not reliable.

The work of Marmarou et al. in 1975 sets the scene for the procedures required to determine an accurate static and dynamic model of the human brain. They measured the distribution of compliance and outflow resistance between cerebral and spinal compartments in anaesthetized, ventilated cats by the analysis of the CSF pressure response to changes in CSF volume. Cerebral and spinal compartments were isolated by inflating a balloon positioned epidurally at the appropriate level. The change of CSF volume per unit change in pressure (compliance) and change of CSF volume per unit of time (absorption) were evaluated by inserting pressure data from the experimental responses into a series of equations developed from a mathematical model [19].

Unfortunately the mathematical complexity of these models made them almost not usable in real clinical approaches. To overcome this, there have been some simpler mathematical models suggested recently by the Ursino research group that can actually be used in clinical procedures [1]. Although the simplification assumptions in the suggested models might lead to some limitations, the models are still able to describe main important aspects influencing ICP. The following sections are dedicated on explanation of some of the most important clinical expressions uses in intracranial pressure research area. The main brain injuries that might lead to elevated intracranial pressures are described briefly. The mechanisms involving in intracranial dynamics are presented in order to provide a good basic knowledge for better understanding of the following chapters.

## 2.2 Basic physiological concepts

As it was mentioned before, while studying the intracranial pressure dynamics and cerebral hemodynamics there are several abbreviations and expressions used in order to pinpoint specific clinical terms in the easiest possible way. The most important ones that were used more often in this research are brought and explained very briefly in the following sections. More detailed information is of course presented in the reference physiology literatures.

### 2.2.1 TBI

TBI (Traumatic Brain Injury) or intracranial injury is caused by an external force such as accident, falling, gunshot or violence and is responsible as the most important cause for death or lifetime disability among children and young populations. As reported by most of physiology literatures almost all of brain injuries are followed by secondary symptoms of damage called secondary brain injury. Secondary brain injury can happen from minutes to hours or days after the initial damage and usually manifests itself in appearance of raised intracranial pressure and variations in cerebral blood flow. Bleeding inside the brain, brain swelling or edema are some of the examples of secondary brain injuries which generally worsens the pathological conditions of the patients such as higher ICP values.

### 2.2.3 ICP

ICP (Intracranial Pressure) the pressure that can be measured within the cranial cavity between the outer membrane (dural) and the brain tissue including the ventricles within the brain and the spinal compartments. ICP reflects different terms such as the blood and CSF volume in the brain, cranial size, the existence of any possible additional mass such as tumor or edema and the dilation or constriction of brain vessels. Average ICP in normal people varies from 7 mmHg to 15 mmHg among adults with normal pathological situations. ICP might rise due to different reasons such as blockage of CSF drainage path, bleeding inside the head, swelling and edema and also due to mass effect which is existence of additional mass such as tumors that take space

inside the brain. Uncontrolled increase in ICP due to pathological conditions (intracranial hypertension) has found to be a main cause for death in patients with severe brain damage or traumatic brain injuries (TBI) [2].

### 2.2.3 ICP monitoring

The method used to measure and monitor the variations of intracranial pressure during different time intervals. Since more than one third of patients suffering from traumatic brain injuries all around the world die due to brain swelling, bleeding or other secondary damages caused by uncontrolled raised pressure in the brain, existence of accurate method in measuring and monitoring this pressure is of high importance. Figure 2.1 shows a typical ICP measurement method which was first suggested by Nils Lundberg in the 1950's. The ICP was measured by an inserted catheter to the lateral ventricle which is connected to an external transducer via a fluid-filled column [20, 21].

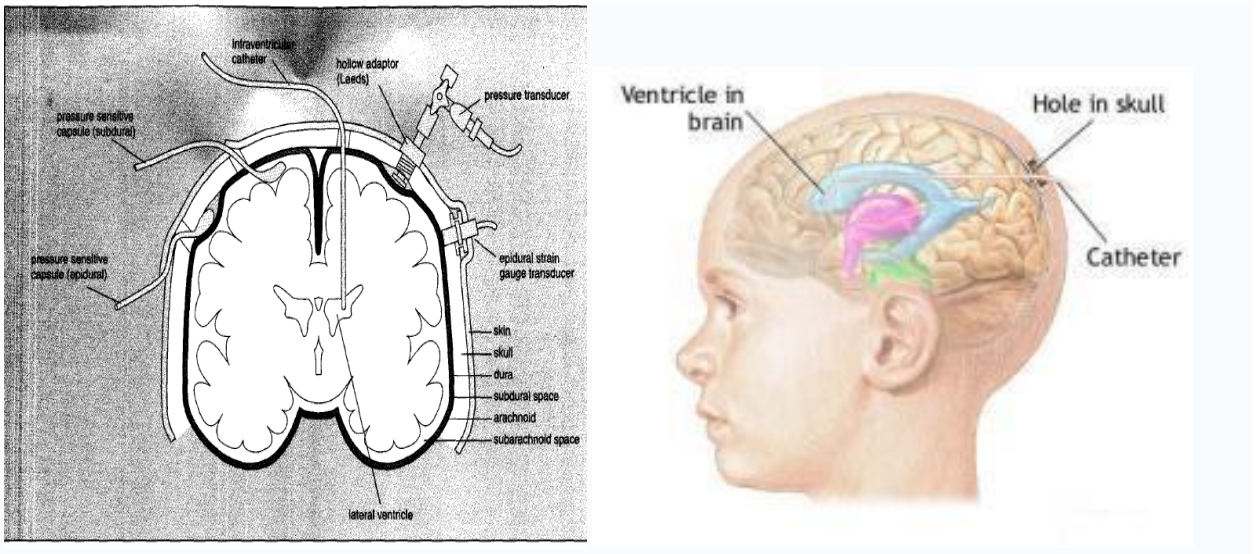


**Figure 2.1: ICP measurement technique. This figure represents the most common invasive method of measuring intracranial pressure via introducing a catheter (implanted strain gauge sensor) into the cranial cavity that has an electrical connection with the outside world and therefore avoid the problems of blockage that can occur with fluid-filled catheters and adaptors. [2]**

### 2.2.4 ABP

ABP (Arterial Blood Pressure) is the blood pressure against the walls in the arteries and vessels. The blood is forced to flow in the vessels by the left ventricle of the heart. This pumping produces a wave form pressure which has its greatest value when the heart ventricle contracts (systolic pressure) and has its lowest value when the ventricle relaxes (diastolic pressure). ABP is measured by millimeters of Mercury and its normal range varies among people with different ages. A young healthy adult ABP must be around 120/80, where the first number represents the

systolic pressure and the second one is the diastolic pressure. Both high blood pressure (hypertension) and low blood pressure (hypotension) are considered to be risky for patients [22].

### 2.2.5 CSF

CSF (Cerebrospinal fluid) is a damping fluid that acts as a buffer for the cortex, in order to protect the brain from mechanical and immunological pressures. CSF circulates over brain stem, the spinal cord and the surface of brain [2].

### 2.2.6 CSF production

CSF is derived by active secretion from cerebral arterial [23, 24, 25]. The site of this process is only conceptually limited to the choroid plexus of the ventricular system. CSF production is a mono-directional procedure, in other words the production in the reverse way is impossible. This is simulated via a diode and a hydraulic production resistance $R_f$. CSF production rate is reported to be constant under normal conditions. The normal average production rate is reported to be around 0.35 ml min−1 and it circulates with the rate of 500 ml day −1 and thus it is renewed 4 to five times a day [2]. This rate is proportional to brain metabolism rate. There have been some methods suggested for measuring CSF production by different authors such as Pappenhaimer. They suggested a method based on constant perfusion of CSF containers with a liquid that contains a tracer but since it's a long time measurement technique, it will average all CSF production dynamics. Therefore there is no really direct accurate procedure for measuring CSF production [26].

### 2.2.7 CSF absorption

Drainage of CSF fluid into the venous compartment takes place predominantly (in humans) through arachnoids granulations that penetrate the walls of the sagittal sinus [27, 28]. It is important to recognize that reverse transport through the arachnoids granulations is impossible, i.e. drainage ceases if subarachnoid ICP is less than sagittal sinus pressure (*P*ss). This is simulated via a diode and a hydraulic production resistance $R_o$.The nature of the venous drainage is linear, i.e. proportional to the pressure gradient between the CSF side of the granulation and the sagittal sinus.

### 2.2.8 CBF

CBF (Cerebral Blood Flow) is the blood supply to the brain in a given time [29].CBF is proportional to the metabolic demand of the brain. If the amount of blood that flows in brain vessels increases more than a certain level, there might be a risk of hyperemia and raised intracranial pressure and subsequent brain tissue damage. In contrast decrease in the blood flow

supply to brain tissues (ischemia) results in brain cells to die gradually if the blood flow decreases more than a certain threshold. In patients with TBI it is of high value for physiologists to keep the CBF level in an appropriate range. Cerebral blood flow is derived and directly proportional with the net pressure of the flow of blood to the brain which is called cerebral perfusion pressure through the following equation

$$CBF = CPP/CVR \tag{2.1}$$

where CVR is the cerebrovascular resistance and CPP is the perfusion pressure which is derived from subtraction of venous pressure from the arterial pressure. On the other hand there is another additional pressure called intracranial pressure that shouldn't be neglected while dealing with pressures inside the brain. It is suggested that the veins in the venous cerebrovascular bed collapse at their entrance into the dural sinuses according to Starling resistor hypothesis. As a result the intravascular pressure of the collapsing section becomes almost the same as the intracranial pressure. Thus CPP can be redefined as the difference between arterial and intracranial pressure according to the following equations [21, 27].

$$CPP = mean(ABP) - mean(ICP) \tag{2.2}$$

### 2.2.9 Compliance and PVI

Assuming an exponential model for the relationship between pressure and volume, compliance is not uniform throughout the pressure range. An expression for compliance was developed by plotting pressure on a logarithmic scale against volume and approximating the transformation by a straight line. The slope of this line was defined as the pressure-volume index (PVI) and is derived by linearization of nonlinear mono-exponential pressure-volume relationship (equation (2.3)), suggested by Marmarou et al. and is the volume needed to cause a tenfold increase in ICP value [19].

$$P_p = P_0 10^{\lambda V} \tag{2.3}$$

$$PVI = \frac{V}{\log_{10}(\frac{P_p}{P_0})} \tag{2.4}$$

Where $P_p$ is the maximum pressure caused by the CSF muck injection and $P_0$ is the initial pressure and V is the volume introduced to the cranium space via the injection.

PVI test is a maneuver used by physiologists to obtain the pressure volume index. This maneuver mostly involves with injection or drainage of muck cerebrospinal fluid into the CSF circulation path via an external tube inserted to the brain through a small hole made in the patients' skull. The reason of injection or drainage of CSF to the brain is to manually perturb the volume inside the cranium space to see its effect according to Monro-Kellie doctrine. Another new suggestion was to insert a balloon instead of muck CSF in order to prevent any infection effect. After the

balloon is inserted it can be blown in order to change the volume and thus the pressure of cranium space inside the brain. Both of CSF muck injection/drainage and balloon injection are considered to be almost dangerous for patients with severe traumatic brain injury due to their possible infection effect and the risk of worst uncontrolled raised pressure inside the brain. By simplifying the equations (2.3) and (2.4) one can obtain

$$\frac{dP}{dV} = \frac{P}{0.4343PVI} \tag{2.5}$$

where $P$ is the pressure change caused by change of volume and can be defined as the inverse of compliance (C) and thus the following equation can be achieved

$$C = \frac{0.4343PVI}{P} \tag{2.6}$$

Thus it can be concluded that the compliance is directly proportional to PVI and inversely proportional to pressure. [21].

The change of volume per unit change of pressure (compliance) and change of volume per unit time (absorption) are intimately related and govern the dynamics of the ICP. When a change in pressure was evoked, values of the initial pressure rise and subsequent recovery yielded data which were used to compute both the compliance and the outflow resistance. For establishment of the pressure-volume curve it is needed to introduce a known volume into the epidural space. It was then shown that by plotting change in volume against $\log_{10} ICP$ an approximate straight line relationship resulted leading to their volume step response method for determining both the compliance and outflow resistance of a compartment. Typical value of compliance from experiments on cats was 0.0257 ml/mm Hg [2].

### 2.2.11 Intracranial elastance coefficient

$K_E$(Intracranial elastance coefficient) is a coefficient first introduced by Avezzat et al and is an index of the rigidity of the craniospinal compartment, inversely proportional to the pressure volume index and compliance [28].

### 2.2.12 Autoregulation

Autoregulation of blood flow is a mechanism which ensures that the perfusion of an organ or vascular bed is maintained fairly constant despite variations in the arterial pressure or better to say perfusion pressure within rather wide limits. Autoregulation is present in most vascular beds and is particularly well developed in the brain. Autoregulation tries to maintain blood flow constancy by dilatation of the resistance vessels when the blood pressure falls and the constriction when the pressure rises. Thus Autoregulation acts like a protection against brain ischemia during blood pressure decrease via vasodilation and prevents capillary damage or edema during pressure increase via vasoconstriction.

According to equation ($CBF = CPP/CVR$) an effective autoregulation tends to keep CBF constant while cerebrovascular resistance varies proportional to perfusion pressure. This is the mechanism through which the body delivers blood and oxygen to the organs that are most highly in need for that. The main concept of Autoregulation is its' being independent of the autonomic nervous system in maintenance of blood flow and that's the reason behind its being named 'auto' regulation. Cerebral Autoregulation is on the other hand the tendency of brain in maintaining appropriate blood pressure inside the brain since it is sensitive to over-perfusion [29].

As an example the autoregulation is the main reason of initial reduction in blood flow followed by gradual increase to the normal level within a short time interval caused by initial drop in perfusion pressure. In patients with weak or impaired Autoregulation the blood flow might not return to the initial value (impaired autoregulation) or might take a long time (slow autoregulation). When the head is injured the cerebral Autoregulation become disturbed resulting in unwanted secondary injuries such as brain swelling followed by raised intracranial pressure [21].

To mention some of the main mechanisms that might be efficient enough to explain the nature of Autoregulation one can name myogenic mechanism, metabolic mechanism, Perivascular nerves and endothelial cell-related factors. In the myogenic mechanism the Autoregulation is mostly based on dilation or constriction of small arteries or arterioles as a response to perfusion pressure variation while the metabolic mechanism changes in metabolic microenvironment are suggested to be responsible for vasomotor response. Perivascular nerves and endothelial cell-related factors are also proposed to play noticeable role in cerebral Autoregulation [30, 31].

### 2.2.13 Brain swelling

As it mostly happens in most of the injuries, the body starts to swell when facing to injury. The brain also swells as a response to different reasons such as TBI, ischemic strokes, brain hemorrhage, tumors and brain infections. Swelling or enlargement of the brain is a secondary injury that might happen due to raised intravascular blood volume (congestive swelling) or tissue water content of the brain (cerebral edema). The main danger in brain swelling is its effect on increasing intracranial pressure which as a result blocks blood to deliver nutrition and oxygen to brain tissues [21].Treatments suggested to prevent further improvement of brain swelling and increase in intracranial pressure mostly depend on the type of the swelling and the reason that caused the swelling. Oxygen therapy, lowering body temperature, lowering intracranial pressure through ventriculostomy (drainage of CSF fluid from inside the brain through a drain tube) or surgery with the aim of removing a part of skull to relieve intracranial pressure (craniectomy) are some of the techniques used by surgeons and medical experts in the case of brain swelling.

### 2.2.14 Monro-Kellie doctrine

A hypothesis based on defining the cranium as a rigid box with a nearly incompressible content, suggesting that the total volume of inside the brain including the brain itself and its blood and cerebrospinal fluid component is constant. This means that any increase in the volume of one of the cranial contents (blood, brain parenchyma and cerebrospinal fluid) due to various pathological conditions or medical treatments leads to a subsequent decrease in the volume of the two remaining compartments. This usually manifests itself in the form of elevated intracranial pressure due to increased volume in the cranium [32].

# Chapter 3

## 3. Mathematical model of interaction between intracranial pressure and cerebral hemodynamics

*During last decades various mathematical models have been suggested by different authors for explaining the interaction between ICP and cerebral hemodynamics. These models might differ in the appearance but they almost have the same physiology and principle behind their equations. In this chapter at first the main model is brought to provide the reader with almost a complete view of the subject of study in this thesis. The main idea behind model's equations and assumptions are explained. The advantages and limitations of the model are discussed and finally the last part is devoted to an extensive explanation of the model that was chosen to be implemented and simulated for this project.*

### 3.1 Qualitative description of the main basic model

The main biomedical principle used in this model is that the craniospinal volume remains constant according to Monro- Kellie doctrine. In other words any change in intracranial volume will lead to an opposite change in the remaining volume [27].

According to Ursino et al. the model of intracranial dynamics can be described by the following electric analogue figure (Figure 3.1). The figure models the intracranial dynamics including small and large arterial segments, capillary and cerebral large veins, bridge veins and lateral lakes, cerebrospinal production and absorption, and finally extra cranial venous pathways [1].

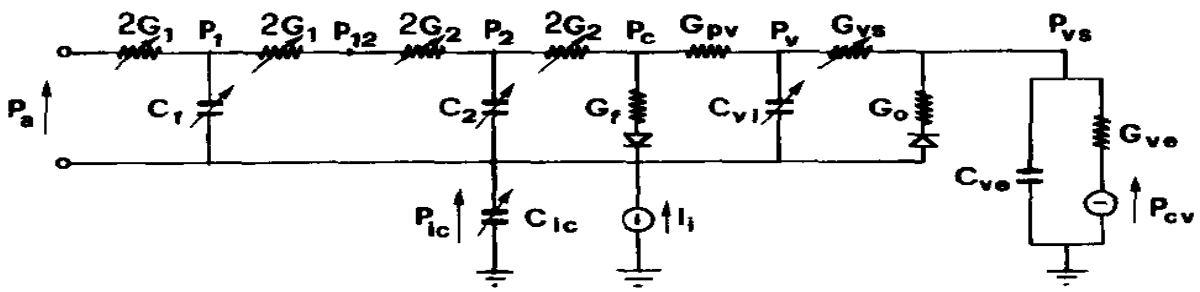


**Figure 3.1: Intracranial dynamics electrical model. $G_{12}$ and $C_{12}$represent large and small arterial vessels conductance and compliance respectively. Pa : arterial pressure; $P_{1,2}$: large and small arteries pressure; $P_c$, $P_v$: capillary and cerebral venous pressure; $P_{vs}$: venous sinus pressure; $P_{cv}$: central venous pressure; $P_{ic}$: intracranial pressure; $G_{pv}$, $C_{vi}$: conductance and compliance of large cerebral veins; $G_{vs}$ : conductance of terminal intracranial veins ; $G_{ve}$, $C_{ve}$:conductance and compliance of the extracranial venous pathways; $G_o$, $G_f$ : conductances to CSF formation and CSF absorption [1].**

### 3.1.1 Model equations

The equations and brief explanations are brought in this chapter, the equations are discussed in a more detailed level of mathematics in relevant articles [32, 33]. The first segment with subscript 1 represents the proximal pial arteries and the second segment with subscript 2 represents the small arterioles. According to Poiseuille law the hydraulic resistances of both of these segments are inversely proportional to the fourth power of inner radius r, thus we have

$$R_j = \frac{K_{Rj}}{r_j^4} \ , G_j = \frac{1}{R_j} \ \ j = 1,2 \tag{3.1}$$

where $r_j$ represents the inner radius of segment j, $G_j$ is the equivalent conductance and finally $K_{Rj}$is a constant parameter. To include the effect of blood volume changes the compliances $C_j$are added for both large and small arteries. The blood volume $V_j$is proportional to the second power of $r_j$ according to

$$V_j = K_{Vj} r_j^2 \tag{3.2}$$

where $K_{Vj}$ is a constant parameter. Thus one can calculate the blood volume changes by differentiating the previous equation and obtain

$$\frac{dV_j}{dt} = 2K_{Vj} r_j \frac{dr_j}{dt} \tag{3.3}$$

Imposing Laplace law in the vessel walls the inner radius of proximal and distal segments can be calculated by

$$P_j r_j - P_{ic}(r_j + h_j) = T_j \tag{3.4}$$

where $P_j$ and $P_{ic}$ are the intravascular pressure and intracranial pressure, the $h_j$ represents cerebrovascular wall thickness and $T_j$ is the wall tension and is composed of three components. These include elastic tension ($T_e$), viscous tension ($T_v$) and muscular tension ($T_m$).

$$T_j = T_{ej} + T_{vj} + T_{mj} \tag{3.5}$$

The first component ($T_{ej}$) is caused by passive elements of the wall and according to different authors is related to elastic stress ($\sigma_e$) trough

$$T_{ej} = \sigma_{ej} h_j \tag{3.6}$$

where $\sigma_{ej}$can be calculated from

$$\sigma_{ej} = \sigma_{0j}\left[e^{(k_{ej}\epsilon_j)} - 1\right] - \sigma_{collj} \qquad \epsilon_j = \frac{r_j - r_{0j}}{r_{0j}} \tag{3.7}$$

$k_{ej}, r_{0j}, \sigma_{collj}$ are all constant parameters. The second component ($T_{vj}$) is dependent on time derivative of wall strain. Thus it can be calculated by

$$T_{vj} = \sigma_{vj} h_j \tag{3.8}$$

Where $\sigma_{vj}$ is driven from

$$\sigma_{vj} = \eta_j \frac{d\epsilon_j}{dt} = \frac{\eta_j}{r_{0j}} \frac{dr_j}{dt} \tag{3.9}$$

Finally the last term ($T_{mj}$) is dependent on the inner radius of the vessel and can be modeled by

$$T_{mj} = T_{m0j}(1 + M_j)\exp(-|(r_j - r_{mj})/(r_{tj} - r_{mj})|^{n_{mj}}) \tag{3.10}$$

where $r_{mj}$ is the inner radius at maximum tension, and $T_{m0j}, r_{tj}, n_{mj}$ are constant parameters. $M_j$ is the so-called activation factor that shows the effect of autoregulation on smooth muscle. For example $M_j > 0$ , shows an active vasoconstriction and $M_j < 0$ shows vasodilation effect.

Wall thickness can be calculated by assuming that vessel wall is incompressible.

$$h_j = -r_j + \sqrt{(r_j^2 + 2r_{0j}\, h_{0j} + h_{0j}^2)} \tag{3.11}$$

$r_{0j}$and $h_{0j}$ represent the inner radius and wall thickness in unstressed conditions.

As it is shown in Figure 3.1, the capillary and cerebral venous segment up to dural sinuses is represented by two conductance ($G_{pv}, G_{vs}$ which are conductance of large cerebral vein and terminal intracranial veins respectively) and one compliance $C_{vi}$ that represents the large cerebral vein compliance. The latter can be calculated by knowing the local transmural pressure through the following equation

$$C_{vi} = \frac{1}{\mathrm{K_v(P_v - P_{ic} - P_{v1})}} \tag{3.12}$$

where $\mathrm{P_v}$ is cerebral venous pressure and $\mathrm{P_{v1}}$is a constant offset parameter. According to Starling resistor hypothesis the terminal intracranial veins section narrows when entering the dural sinus. Thus the conductance at dural sinus level can be calculated by

$$C_{vs} = C'_{vs} \frac{\mathrm{P_v - P_{ic}}}{\mathrm{P_v - P_{vs}}} \tag{3.13}$$

Where $\mathrm{P_{vs}}$is the venous sinus pressure. $C'_{vs}$ is a constant parameter. According to exponential relationship between intracranial pressure and volume the intracranial compliance is formulated by this equation

$$C_{ic} = \frac{1}{K_E . P_{ic}} \tag{3.14}$$

where $K_E$ is the elastance coefficient. The remaining part is model of CSF production and absorption which is represented through conductance $G_f, G_o$with diodes to show the mono-directionality of each procedure. The last segment represents the extracranial venous pathways through a parallel system of conductance ($G_{ve}$) and compliance ($C_{ve}$).

Imposing mass preservation on the nodes in the electrical diagram in Figure3.1 we can obtain the following equations

$$G_1(P_a - P_1) - \frac{G_1 G_2}{G_1 + G_2}(P_1 - P_2) = \frac{1}{2}\frac{dV_1}{dt} = K_{V1} r_1 \frac{dr_1}{dt} \tag{3.15}$$

$$\frac{G_1 G_2}{G_1 + G_2}(P_1 - P_2) - G_2(P_2 - P_c) = \frac{1}{2}\frac{dV_2}{dt} = K_{V2} r_2 \frac{dr_2}{dt} \tag{3.16}$$

$$2G_2(P_2 - P_c) - G_{pv}(P_c - P_v) = G_f(P_c - P_{ic})h(P_c - P_{ic}) \tag{3.17}$$

$$G_{pv}(P_c - P_v) - G_{vs}(P_v - P_{vs}) = C_{vi}\left(\frac{dP_v}{dt} - \frac{dP_{ic}}{dt}\right) \tag{3.18}$$

$$G_{vs}(P_v - P_{vs}) + G_o(P_{ic} - P_{vs})h(P_{ic} - P_{vs}) = G_{ve}(P_{vs} - P_{cv}) + C_{ve}\frac{dP_{vs}}{dt} \tag{3.19}$$

where h () is the Heaviside step function and represents the uni-directinality of CSF production and absorption. According to the Monro-Kellie doctrine the overall volume of craniospinal cavity is constant. Thus one can obtain

$$C_{ic}\frac{dP_{ic}}{dt} = 2K_{V1} r_1 \frac{dr_1}{dt} + 2K_{V2} r_2 \frac{dr_2}{dt} + G_f(P_c - P_{ic})h(P_c - P_{ic}) + C_{vi}\left(\frac{dP_v}{dt} - \frac{dP_{ic}}{dt}\right)$$

$$-G_o(P_{ic} - P_{vs})h(P_{ic} - P_{vs}) + I_i \quad (3.20)$$

where $I_i$ is the rate of CSF mock injection. Small and proximal arteries are controlled by two distinct mechanisms. The proximal arteries are assumed to be controlled by pressure dependent regulatory mechanism while the small arterioles are controlled by flow-dependent mechanism. This is described through the following equations [34, 35].

$$\frac{dM_1}{dt} = -\frac{1}{\tau_1}M_1 + \frac{1}{\tau_1}\frac{2}{\pi}atan[H_1(P_a - P_{an} - P_v + P_{vn})] \quad (3.21)$$

$$\frac{dM_1}{dt} = -\frac{1}{\tau_2}M_2 + \frac{1}{\tau_2}\frac{2}{\pi}\ atan(H_2\frac{q-q_n}{q_n}) \quad (3.22)$$

where $\tau_j, H_j$ (for j=1,2) are used to represent the time constant and the gain of feedback mechanism for both proximal and distal sections. According to Ursino et al. the arctg function is used to show the upper and lower limits for cerebral autoregulation [1]. Here q is used to represent the cerebral blood flow and can be calculated by the following equation

$$q = 2G_2(P_2 - P_c) \quad (3.23)$$

Where $q_n$denotes the condition when autoregulatory mechanisms are at their maximum strength.

### 3.1.2 Inputs and parameters of the model

The model is fed with three inputs: SAP (or ABP as arterial blood pressure), $P_{cv}$ (central venous pressure) and rate of CSF mock injection ($I_i$). The model parameter choice is based on two conditions.

1. Parameters that show noticeable alteration during TBI
2. Parameters that ICP shows a great sensitivity to their variation

Thus considering the mentioned conditions the parameters are chosen to be

- $K_G = \frac{G_o}{G_f}$
- $K_E$
- $\tau_2, H_2$

This agrees with the previous studies for modeling ICP dynamics, moreover this model adds the effect of cerebral hemodynamic change and cerebral blood volume change on ICP (last parameter*s* $H_2\ , \tau_2$). The reason why the first parameter is described by the ratio of CSF production over CSF absorption is that these two terms cannot be identified independently with

good accuracy. The reason behind choosing only $H_2$ , $\tau_2$ as the last parameters and ignoring $H_1$ , $\tau_1$ is the small effect of proximal arteries on ICP during PVI (pressure-volume-index) tests. Thus $H_1$ is assumed to be zero. In other words the blood volume changes are related to only small arterioles in this model.

## 3.2 Simplified model used for the aim of simulation

Now the model that is chosen to be implemented and simulated for the aim of this project is discussed below. The reason for this choice was mostly based on its comparable simplicity of equations and also the availability of the clinical data needed as input to run the model. This model is based on the previous suggested model by Ursino et.al which is simplified through employing two main assumptions [32]. The good thing about this reduction is that although the whole physiological procedure is described in a much simpler way, noticeable malfunctioning of the model was not observed.

### 3.2.1 Main simplification assumptions

The main simplification assumptions implemented to the previous model which leads to this new simple model are as follows.

a) There is no distinguishable boundary between proximal and distal arterial-arteriolar segments. This means that both conductance (G1, G2) are simplified to a new regulated arterial resistance Ra which is responsible for pressure drop and both compliances (C1, C2) are integrated in a regulated arterial compliance Ca which is responsible for storing certain amount of blood volume in itself.
b) Since venous cerebrovascular bed behaves like a Starling resistor [36] ,which narrows in the terminal of intracranial veins by a small increase in ICP, the pressure of large cerebral vein is assumed to be the same as ICP [27]. Thus there would be no more compliance since due to this assumption the gradient pressure between large cerebral vein and intracranial pressure (transmural pressure) remains constant and blood volume changes are not noticeable.

### 3.2.2 Advantages of simplified model

The advantage of this simplification can be summarized in two main aspects. First the number of parameters is reduced. This means that the model is able to present the whole physiological procedure through a few numbers of parameters and also the parameter identification process becomes faster [27]. Second advantage is that the system becomes a second order one having ICP and Ca as its states. This reduction in number of states will make it much easier to do the stability analysis study for the model.

### 3.2.3 Qualitative description of simplified model

Similar to the previous model the simplified model contains three segments including arterial-arteriolar cerebrovascular bed, venous cerebrovascular bed and CSF circulation path, CSF formation at capillary level to CSF re-absorption and dural sinus.

#### 3.2.3.1 Arterial- arteriolar cerebrovascular bed

As mentioned in the simplification assumptions section this segment has been simplified into a hydraulic resistance $R_a$ and hydraulic compliance $C_a$. The first is responsible for pressure drop through the arterial cerebrovascular bed and the latter can store a certain amount of blood volume in itself. Equations of this model can be derived from writing mass preservation principle for both nodes 1 and 2 in the analogue electric Figure 3.2. Assuming certain relationships among CBV, cerebrovascular resistance and autoregulation mechanism helps to add auxiliary equations.

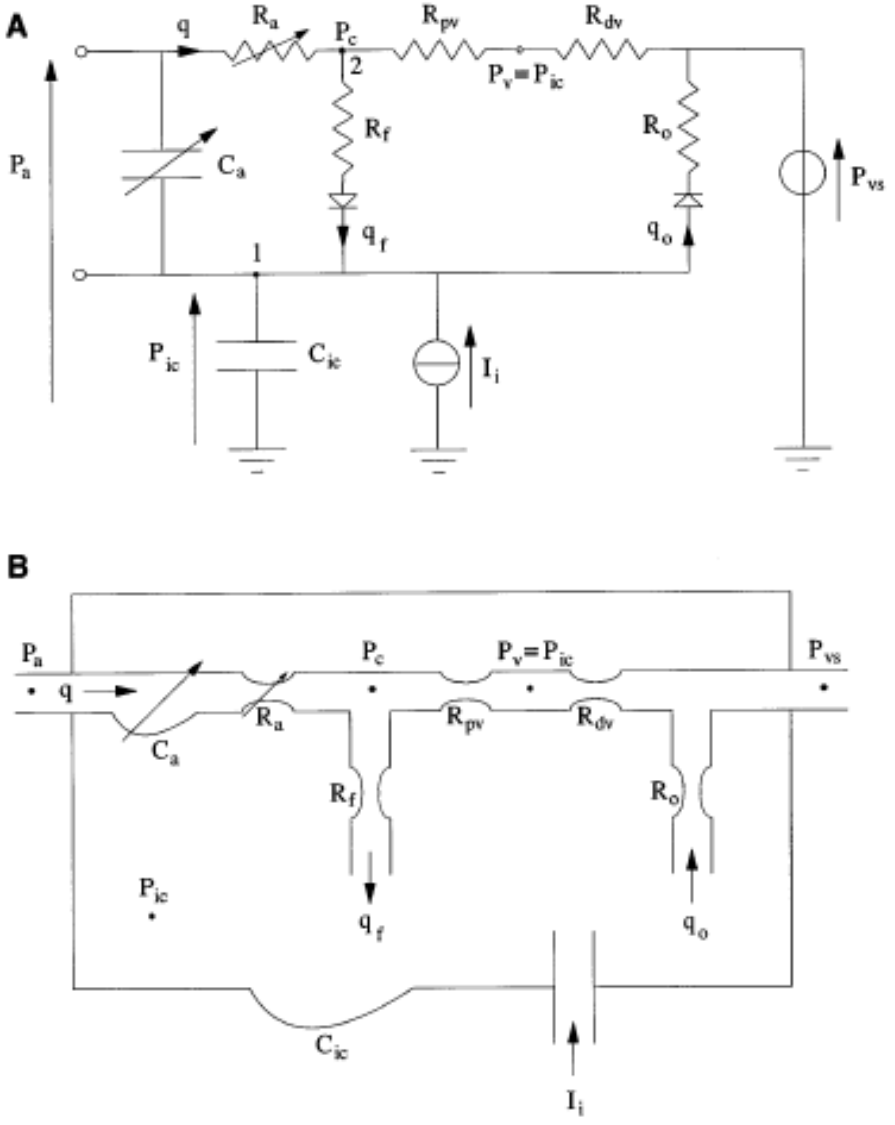


**Figure 3.2: Electric analog (A) and corresponding mechanical analog (B) of intracranial dynamics. CBF (q) enters the skull at the arterial pressure. At the arterial-arteriolar segment hydraulic autoregulatory resistance ($R_a$) is responsible for the pressure drop and arterial-arteriolar compliance is responsible for storing blood volume. CSF is produced at capillary pressure ($P_c$) through a mono-directional path from CSF formation resistance ($R_f$) The venous cerebrovascular bed is represented by proximal venous resistance ($R_{pv}$), collapsing segment resistance ($R_{dv}$). According to Stariling resistor the central venous pressure ($P_V$) is assumed to be the same as ICP. Then CSF is reabsorbed under the venous sinus pressure ($P_{vs}$) through a mono-directional path from outflow resistance ($R_o$). The intracranial compliance is finally represented by $C_{ic}$and is responsible for maintaining the balance between CSF inflow ($q_f$), CSF outflow ($q_o$) and blood volume changes in arterial capacity. [1].**

The arterial-arteriolar blood volume($V_a$) is related to pressure gradient according to

$$V_a = C_a.(P_a - P_{ic}) \tag{3.24}$$

In which $P_a$ is the normal arterial blood pressure or the available patient ABP data measured in hospital and $P_{ic}$ is the intracranial pressure which is also measured at hospital through the invasive method and the model is supposed to produce and simulate it.

By differentiating equation (3.24) we have

$$\frac{dV_a}{dt} = C_a.\left(\frac{dP_a}{dt} - \frac{dP_{ic}}{dt}\right) + \frac{dC_a}{dt}.(P_a - P_{ic}) \qquad (3.25)$$

As it is obvious from the equation the change of arterial-arteriolar blood volume is made of two distinct terms. First is the change due to passive transmural pressure variation. The second term represents the active change induced by autoregulation control mechanism.

In order to describe the second term in equation (3.25) which is the influence of autoregulatory mechanism on the arterial-arteriolar compliance ($C_a$), the procedure has been simplified in three stages shown in block diagram of Figure 3.3.

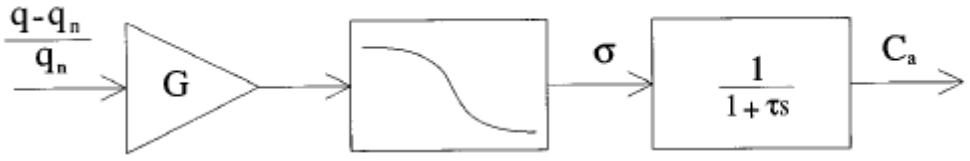


**Figure3. 3: Block diagram of action of autoregulatory mechanism on arterial-arteriolar compliance, $C_a$ (hence on arterial blood volume), in response to given percent change in CBF ($\frac{q-q_n}{q_n}$). First block represents the central autoregulation gain, G. Second block describes static sigmoidal autoregulation response, with lower and upper limits. Third block simulates the autoregulation dynamics by a low-pass transfer function with time constant τ [1].**

$$\frac{dC_a}{dt} = \frac{1}{\tau}.[-C_a + \sigma(G.x)] \qquad (3.26)$$

where τ is the time constant of regulation and $\sigma(G.x)$ represents the sigmoidal autoregulation curve and is a function of autoregulation gain (G), nominal value for arterial compliance ($C_{an}$) and CBF percent change (x). This curve has two saturation levels with upper and lower limits which are presented through small variations ($\frac{\Delta C_a}{2}$) around the nominal value. As it is obvious from the electric analogue figure the cerebrospinal flow (CBF) can be calculated by

$$q = \frac{P_a - P_c}{R_a} \qquad (3.27)$$

Having the CBF value, the CBF percent change (x) normalized to the nominal value $q_n$ can be calculated by

$$x = \frac{q - q_n}{q_n} \tag{3.28}$$

where $q_n$is defined to be the value of CBF needed by tissue metabolism. Finally the sigmoidal autoregulation curve is represented by the following equation.

$$\sigma(G.x) = \frac{(C_{an} + \frac{\Delta C_a}{2}) + (C_{an} - \frac{\Delta C_a}{2}).\exp\left(G.\frac{x}{K_\sigma}\right)}{1 + \exp\left(G.\frac{x}{K_\sigma}\right)} \tag{3.29}$$

where $K_\sigma$ is a constant parameter used for adjusting the curve slope. $K_\sigma$ should be chosen in a way to set the central slope of the curve at $-G$. Thus according to $\frac{d\sigma}{dx}|_{x=0} = \frac{-G\Delta C_a}{4K_\sigma}$ the $K_\sigma$ is chosen to be $\frac{\Delta C_a}{4}$ . Since increase in blood volume during vasodilation is more than the decrease during vasoconstriction, depending on decrease or increase in CBF amount and thus the sign of x, $K_\sigma$ takes different values. If the CBF increases ($x > 0$) the arterial compliance would decrease due to vasoconstriction and vice versa. This is explained by the following expressions.

$$\begin{cases} x < 0 \rightarrow \Delta C_a = \Delta C_{a1} \; ; \; K_\sigma = \frac{\Delta C_{a1}}{4} \\ x > 0 \rightarrow \Delta C_a = \Delta C_{a2} \; ; \; K_\sigma = \frac{\Delta C_{a2}}{4} \end{cases} \tag{3.30}$$

Moreover considering the arterial-arteriolar segment as a microvascular bed that consists of several microvessels with equal inner radius *r*, according to Hagen-Poiseuille law the volume would be directly proportional to $r^2$, thus the hydraulic resistance of the arterial-arteriolar segment will be inversely proportional to $r^4$ through the following equation

$$R_a = \frac{K'_R}{r^4} = \frac{K_R . C_{an}^2}{V_a^2} \tag{3.31}$$

where $K_R$ is a constant parameter. This means that any increase in arterial-arteriolar blood volume due to vasodilation leads to a decrease in arterial-arteriolar resistance and vice versa.

#### *3.2.3.2 Venous cerebrovascular bed*

This includes two segments; the first (proximal) segment from cerebral capillaries down to the lateral lacunae or lakes and the bridge veins is described by means of a hydraulic resistance ($R_{pv}$). The second part is the segment downstream of the bridge veins and is represented through a hydraulic resistance ($R_{dv}$). In this model according to the starling resistor behavior, collapsing at the entrance into dural sinuses and thus equal pressure of the collapsing segment to ICP, the second segment has not been mentioned in the equations [27]. Moreover, there would be no more venous compliance since the transmural pressure between large cerebral veins and ICP remains quite constant.

### *3.2.3.3 CSF Circulation*

Cerebrospinal fluid is assumed to be produced at the level of cerebral capillaries and absorbed at the dural sinuses. The production is modeled through a CSF formation resistance ($R_f$) and the absorption is represented through a CSF outflow resistance ($R_o$). The diodes are used in order to show the uni-directionality of these procedures. In other words CSF is only produced downwards direction from cerebral capillaries and reabsorbed upwards through the dural sinuses. The last segment is the dural sinus pressure ($P_{vs}$) which is given as input to this model and should be less than ICP in order to have no conflict with the Starling resistor hypothesis.

As mentioned before the overall volume in the craniospinal space is assumed to be constant according to Monro-Kellie doctrine. Thus any change in intracranial volume will lead to an opposite change in the remaining volumes. To simply show the overall constancy of craniospinal volume one can write the mass preservation principle at node 1. This gives the following equation

$$C_{ic}\frac{dP_{ic}}{dt} = \frac{dV_a}{dt} + \frac{P_c - P_{ic}}{R_f} - \frac{P_{ic} - P_{vs}}{R_o} + I_i \tag{3.32}$$

where $C_{ic}$ is the intracranial capacity, which is responsible for storing a certain amount of volume. According to mono-exponential pressure-volume relationship that has been suggested by different authors such as Marmarou et al. and Avezaat et al., this capacity is proportional to ICP via the following equation [37, 38].

$$C_{ic} = \frac{1}{K_E.P_{ic}} \tag{3.33}$$

In this equation $K_E$ represents the intracranial elastance coefficient introduced by Avezaat et al and defines how rigid the craniospinal compartment can be. This is the inverse form of PVI index that has been suggested by Marmarou et al [39,40].

Writing the mass preservation principle at node 2 will give us the following equation.

$$\frac{P_a - P_c}{R_a} = \frac{P_c - P_{ic}}{R_f} + \frac{P_c - P_{ic}}{R_{PV}} \tag{3.34}$$

As it is written in the equation, the cerebral venous pressure is substituted by intracranial pressure according to the Starling resistor mechanism.

These equations are then integrated in order to simplify the whole model into a second order system with two states intracranial pressure (ICP) and arterial-arteriolar compliance ($C_a$). The input quantities contain arterial pressure ($P_a$), arterial pressure time derivative ($\frac{dP_a}{dt}$), venous sinus pressure ($P_{vs}$) and the rate of mock CSF injection or withdrawal from the cranial cavity.

According to the data collected at hospital, the first input ($P_a$) can be easily measured but there is no exact measurement technique for $P_{vs}$. On the other hand clinical experiment has suggested that CSF mock injection is a very risky procedure especially for patients suffering from traumatic brain injury. Thus $P_{vs}$ is given the nominal value of 6 mmHg according to what has been

suggested by Ursino et al [1] and Ii is neglected due to the absence of CSF mock injection procedure.

### 3.2.4 Feedbacks of the model

As shown in Figure 3.4 this model has 4 feedback loops. According to our analytical knowledge negative feedbacks tend to stabilize the output while positive feedbacks might lead the output to become unstable. This instability might show itself by self sustained oscillations. This is more discussed in the stability analysis section.

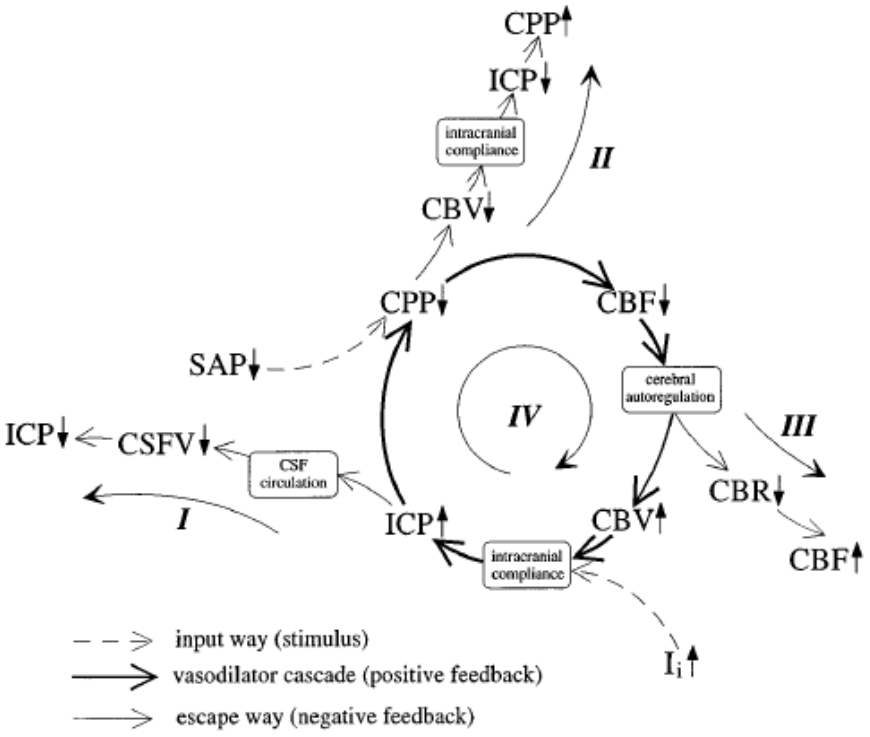


**Figure 3.4: Models feedbacks. Here different feedbacks in the model are represented. Negative feedbacks are shown by escape ways, the first one is caused by CSF circulation and CSF volume change (CSFV). Feedback 2 is a result of passive blood volume changes. The third feedback explains the autoregulation control effect on CSF through the cerebrovascular resistance (CBR) alterations. Finally the positive feedback (feedback 4) is imputable to active CBV changes due to autoregulation. This feedback was suggested by Rosner and is called vasodilatory cascade. Since the 4th feedback is a positive one, it might lead to instability of ICP which can manifest itself through self sustained oscillations [1].**

For now let us concentrate on different reasons for both positive and negative feedbacks. The negative feedbacks are resulted from CSF circulation (feedback 1), CBV change effect on ICP (feedback 2) and autoregulation effect on CBF (feedback 3). According to Rosner, the positive feedback (feedback 4) is caused by active arterial-arteriolar blood volume changes and is called 'vasodilatory cascade' [41]. This can be explained by a procedure of reduction in cerebral

perfusion pressure (CPP= SAP -ICP) that leads to vasodilation and thus increase in CBV followed by a rise in ICP. This will cause a secondary reduction in CPP and will continue until the maximum vasodilation is reached. Except the self-sustained oscillations or limit cycles the other possible consequence is production of paradoxical response. This means that the system has a delay in responding to small initial perturbations [41, 42, 43].The complete analysis of both phenomena is brought in the stability analysis chapter. The values chosen for parameters nominal values and the reasons behind each assumption, results for sensitivity and stability analysis are completely discussed in the following chapters.

# Chapter 4

## 4. Stability analysis

*This chapter includes discussions about the main reasons for occurrence of self sustained oscillations as a result of ICP instability, analytical study involving finding systems equilibrium point and linearization of equations around that, finding systems Jacobian matrix and characteristic equation for computation of eigenvalues and bifurcation diagrams.*

### 4.1 Positive feedback and instability

As mentioned the existence of positive feedback, called 'vasodilatory cascade', might be a reason leading to instability of intracranial pressure. A rise in ICP will cause a parallel increase in cerebral venous pressure according to Starling resistor behavior. Thus the cerebral perfusion pressure decreases accompanied by a vasodilation. As a consequence CBV would increase and a delayed secondary ICP rise would happen. Impaired CSF circulation (high values for $R_o$), low intracranial compliance (high values for $K_E$) and also high values for autoregulation gain (G) are some of the examples of conditions that might result in ICP instability [42].

As far as the 'vasodilatory cascade' is compensated by the compensatory mechanisms such as efficient intracranial compliance (elasticity $K_E$) and CSF outflow ($R_o$), the system keeps its stability and therefore no oscillation would occur [42]. There is a threshold when the compensatory system is not efficient enough to neutralize the vasodilatory cascade. This is the time that ICP instability starts to appear in the form of so-called A wave oscillations [32, 33]. As it's well known instability can manifest itself through self-sustained oscillations. The same thing happens when dealing with unstable intracranial pressure. The oscillation waves have a great similarity with the ones introduced as Lundberg A waves or plateau waves [20]. Figure 4.1 is an example of how ICP time pattern when it becomes unstable.

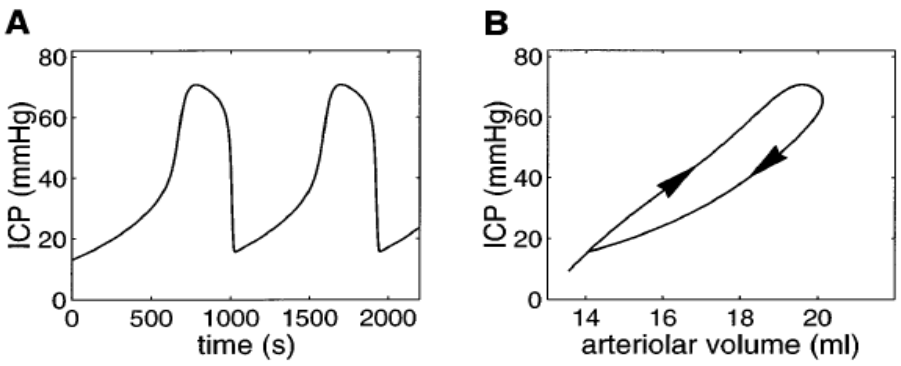


**Figure 4.1: ICP Instability results; A: plateau waves (A waves) of ICP caused by increase in Ro (12 times) and increase in $K_E$ (two times) is shown. B: the ICP variation vs arterial volume changes creates a closed loop called limit cycle [1].**

Moreover, as mentioned before these oscillations are self-sustained. In other words the oscillation can happen only due to intrinsic instability and there is no need for external stimuli in order for the model to exhibit oscillations. Having said that, external perturbations such as hypotension, SAP decrease, might help to facilitate the generation of A waves when the system is close to instability boundary [1, 41]. The following section gives a brief summary of mathematics behind stability analysis.

## 4.2 Simplification of the model

To simplify the model according to equation (3.34) Pc can be calculated from this formula

$$\frac{P_a - P_c}{R_a} = \frac{P_c - P_{ic}}{R_f} + \frac{P_c - P_{ic}}{R_{PV}} \tag{4.1}$$

The left hand side term represents the cerebrospinal flow (CBF) and the first right hand side of the equation stands for CSF production rate. Since the latter term is much smaller than q (CBF), one can simplify the previous equation

$$P_c = \frac{P_a . R_{PV} + P_{ic} . R_a}{R_{PV} + R_a} \tag{4.2}$$

The other simplification that can be done is to integrate equations (3.32), (3.33) and (3.34).Thus we obtain

$$\frac{dP_{ic}}{dt} = \frac{K_E . P_{ic}}{1 + C_a . K_E . P_{ic}} \left[ C_a \frac{dP_a}{dt} + \frac{dC_a}{dt} . (P_a - P_{ic}) + \frac{P_c - P_{ic}}{R_f} - \frac{P_{ic} - P_{vs}}{R_o} + I_i \right] \tag{4.3}$$

## 4.3 Approach to stability analysis problem

At this level of study the aim is to find out when the system is stable and when it's not. In other words the goal is to trace the boundary at which the system changes its behavior from stability to instability. The stability means that the system settles down at a steady-state level and instability means that the system exhibits self-sustained oscillations like plateau waves which were introduced by Lundberg and called A-waves [20].

Some of the most important conditions leading to instability of ICP according to Ursino et al. are decrease in CSF outflow and decrease in intracranial compliance. In other words increase in $K_E$ (elastance coefficient) and $R_o$ (CSF outflow resistance) are conditions that are favorable for instability of the system [1, 32].

Based on the parameter values ($R_o$, $K_E$ and G), the generated eigenvalues can be real negative (stable), complex with positive real parts (unstable) and imaginary (boundary between being stable and unstable). The most interesting area for the purpose of this research could be the one that the system is close to the boundary of being unstable. The reason is that in this condition a small perturbation might lead to instability of the system manifesting itself in a self-sustained oscillation or paradoxical response. A Hopf bifurcation diagram is a diagram used to differentiate between the stable and unstable region based on the parameter values and set a boundary between them. This can provide us with a good understanding of in what way the parameter value alteration might lead to instability and could be useful for experts in choosing right treatments when even a small perturbation might worsens the patient's condition. For this aim, the model is linearized with respect to the equilibrium point to find the Jacobian matrix, eigenvalues and finally the parameter values at which the model becomes unstable.

## 4.4. Stability analysis and bifurcation diagrams

According to the model's equations, one can simplify them into

$$\begin{cases} \frac{dx}{dt}(t) = f(X(t), V(t), u(t); \Theta) \\ g(X(t), V(t), u(t); \Theta) = 0 \end{cases} \tag{4.4}$$

Where *f* consists of the two state variables derivatives including:

$$\frac{dP_{ic}}{dt} = \frac{K_E \,.P_{ic}}{1+C_a \,.K_E \,.P_{ic}} \left[ C_a \frac{dP_a}{dt} + \frac{dC_a}{dt} . (P_a - P_{ic}) + \frac{P_c - P_{ic}}{R_f} - \frac{P_{ic} - P_{vs}}{R_o} + I_i \right] \tag{4.5}$$

$$\frac{dC_a}{dt} = \frac{1}{\tau} . [-C_a + \sigma(G.x)] \tag{4.6}$$

and *g (.) = 0* represents a system of auxiliary equations derived from

$$V_a = C_a.(P_a - P_{ic}) \quad (4.6)$$

$$R_a = \frac{K'_R}{r^4} = \frac{K_R.C_{an}^2}{V_a^2} \quad (4.7)$$

$$P_c = \frac{P_a.R_{PV} + P_{ic}.R_a}{R_{PV}+R_a} \quad (4.8)$$

$$q = \frac{P_a - P_c}{R_a} \quad (4.9)$$

$$x = \frac{q - q_n}{q_n} \quad (4.10)$$

$$\sigma(G.x) = \frac{(C_{an}+\frac{\Delta C_a}{2})+(C_{an}-\frac{\Delta C_a}{2}).\exp(G.x/K_\sigma)}{1+\exp(G.x/K_\sigma)} \quad (4.11)$$

As shown in the equation (4.4) the function has 4 variables. The first category is the state variables vector X(t) ,the second one would include the auxiliary variables vector V(t) that are dependent on both input and state variables, the third group is the input quantities vector U(t) and the last one is model parameters vector Θ.

$$X(t) = [P_{ic}, C_a]^T \quad (4.12)$$

$$V(t) = [V_a, R_a, P_c, q, x, \sigma]^T \quad (4.13)$$

$$U(t) = \left[P_a, \frac{dP_a}{dt}, P_{vs}, I_i\right]^T \quad (4.14)$$

$$\Theta = \left[R_o, R_f, R_{pv}, K_E, K_R, G, q_n, \tau, \Delta C_a, C_{an}\right]^T \quad (4.15)$$

The next step is to find equilibrium points by introducing a set of constant input and parameters values (U0 and Θ) to the system of equation (4.15). U0 is obtained by setting the $P_a$, $P_{vs}$values to their nominal values (100 mmHg and 6 mmHg respectively) and $\frac{dP_a}{dt}$ would become zero by assigning a constant value to $P_a$and $I_i$ is also set to zero based on absence of any mock CSF withdrawal or injection. Θ is also obtained by setting all parameters to their nominal values except the ones that are used to find the boundary. This means that by the given input and parameter values there would be an equilibrium point in which the mentioned equation becomes

$$\begin{cases} f\left[X_0(U_{0,}\Theta), V(U_{0,}\Theta), U_0; \Theta\right] = 0 \\ g\left[X_0(U_{0,}\Theta), V(U_{0,}\Theta), U_0; \Theta\right] = 0 \end{cases} \quad (4.16)$$

where $\left[X_0(U_{0,}\Theta), V(U_{0,}\Theta)\right]^T$ is the only equilibrium point at Uo and Θ. By linearizing it around the equilibrium point we obtain

$$\begin{cases} \frac{dx}{dt} = A(X - X_0) + B(V - V_0) + C(U - U_0) \\ D(X - X_0) + E(V - V_0) + F(U - U_0) = 0 \end{cases} \quad (4.17\text{ a, b})$$

where

$$A = \left[\frac{\partial f}{\partial X}\right]_0, B = \left[\frac{\partial f}{\partial V}\right]_0, C = \left[\frac{\partial f}{\partial U}\right]_0 \quad (4.18)$$

$$D = \left[\frac{\partial g}{\partial X}\right]_0, E = \left[\frac{\partial g}{\partial V}\right]_0, F = \left[\frac{\partial g}{\partial U}\right]_0$$

By integrating both equations in (4.17 a, b), we will have

$$\frac{dx}{dt} = (A - BE^{-1}D)(X - X_0) + (C - BE^{-1}F)(U - U_0) \quad (4.19)$$

As it is well known in mathematics the Jacobian matrix of an equation needs to be defined in order to describe how the function varies by small variation in its variables (state values in this case) through a linear approximation. This can be done by finding the first-order partial derivatives of that function at a given point which in this case is the equilibrium point. The general form of the Jordan matrix is

$$J = \begin{bmatrix} \frac{\partial f1}{\partial X1} & \cdots & \frac{\partial f1}{\partial Xn} \\ \cdots & & \cdots \\ \frac{\partial fm}{\partial X1} & \cdots & \frac{\partial fm}{\partial Xn} \end{bmatrix} \quad (4.20)$$

From equation (4.19) the Jacobian matrix is

$$J(X_0, V_0) = \begin{bmatrix} J_{11} & J_{12} \\ J_{21} & J_{22} \end{bmatrix} = \mathrm{A} - BE^{-1}D \quad (4.21)$$

Thus for variable $\lambda$ we obtain the characteristic equation

$$\lambda^2 - \lambda(J_{11} + J_{22}) + \mathrm{Det\,(J)} = 0 \quad (4.23)$$

The interesting condition for the aim of this study appears only when the $(J_{11} + J_{22})$ value is equal to zero and thus the eigenvalues equation would become

$$\lambda^2 + \mathrm{Det\,(J)} = 0 \quad (4.24)$$

$$\lambda^2 = -\mathrm{Det\,(J)},\ \lambda_{1,2} = \pm j\omega$$

As far as Det(J) is a positive value the eigenvalues become imaginary ones. These are exactly the eigenvalues that produce the stability/instability boundary. The model was finally evaluated for a wide range of $R_o$ and $K_E$ and the checking condition of $(J_{11} + J_{22}) = 0$. Figure 4.2 shows that for all assigned values of $R_o$ and four different values of $K_E$ how the Jacobian condition varies. As it can be understood from this figure for some values of $K_E$ and $R_o$ the Jacobian condition is

met and becomes equal to zero. These parameter values are saved and plotted afterwards as presented in Figures 4.3, 4.4 and 4.5.

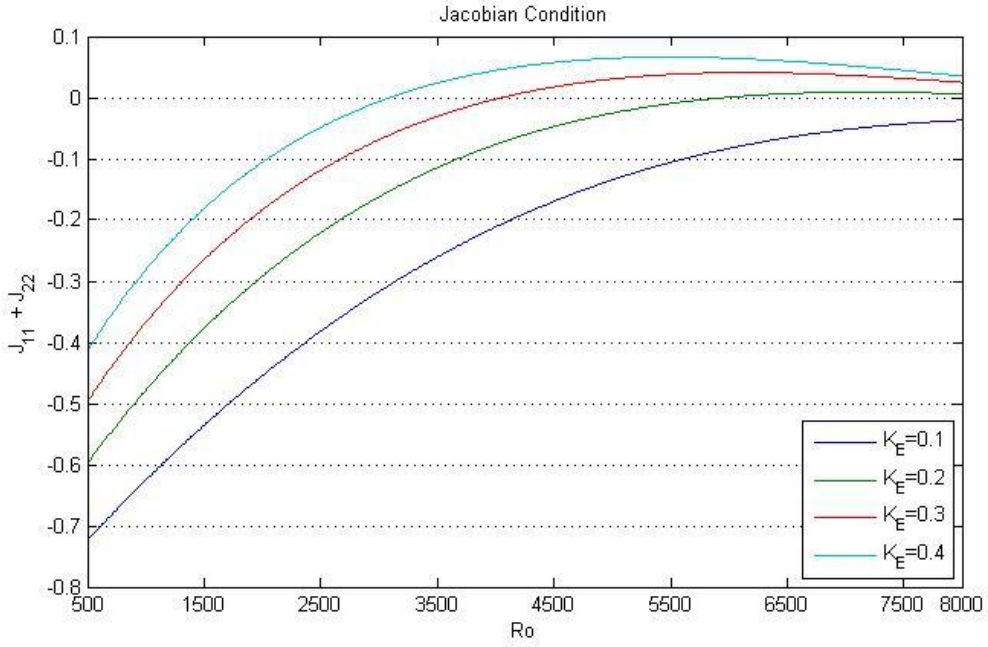


**Figure 4.2: Jacobian condition. This figure shows the values for Jacobian condition ($J_{11} + J_{22}$) for a reasonable range of $R_o$and four values of $K_E$ (0.1, 0.2, 0.3, 0.4 $ml^{-1}$)**

Bifurcation is a mathematical term used for the particular critical parameter values at which the models stable equilibrium point becomes unstable and the model changes its topological structure of trajectories [44, 45, 46, 47]. As mentioned, being aware of exactly at which conditions a little perturbation might lead to ICP instability is of high value. As mentioned before, for a better understanding of what conditions or parameters values cause one stable equilibrium point to become unstable, Hopf bifurcation diagram was used.

The same input of $U_0$ , $\Theta$ are set to the nominal values except the parameters used to obtain the bifurcation boundary. A Hopf bifurcation diagram as shown in the next two following figures is a tool that can be used to differentiate between the stable and unstable region by creating a boundary between them which is obtained from checking the Jacobian condition for different parameter values. Figures 4.3 and 4.4 show that the model becomes unstable when CSF outflow resistance and intracranial elastance coefficient are both increased significantly. In other words the bifurcation curve shows the set of pair $R_o$ and $K_E$ values that meet the Jacobian condition mentioned above. Accordingly there are different combinations of $R_o$ and $K_E$ that lead to instability. The same procedure can be applied to see the effect of autoregulation gain with

respect to CSF outflow resistance. This time the G values have been changed with respect to $R_o$ values in order to find the instability boundary. Again it's obvious from the figure that high values of autoregulation gain accompanied by high values of CSF outflow resistance lead to model to become unstable.

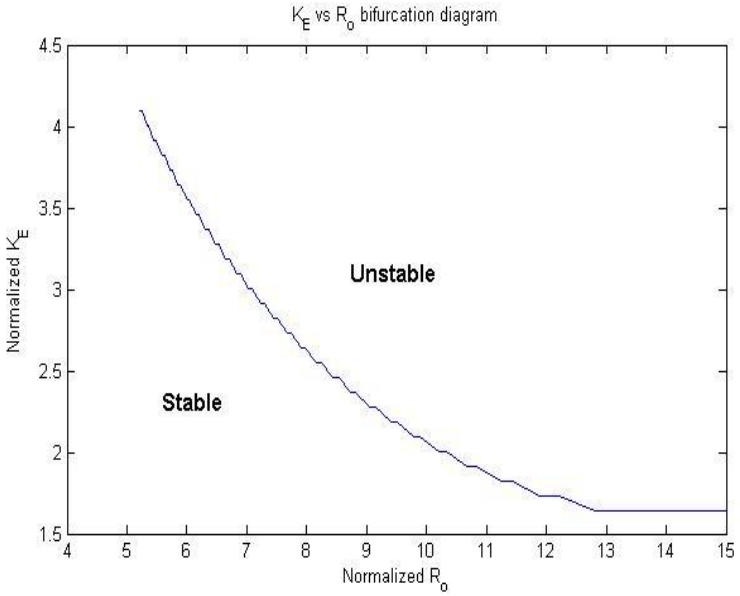


**Figure 4.3: Bifurcation diagram describing relationship between $K_E$and $R_o$. The boundary between stability and instability is obtained by assigning different values to parameters $K_E$and $R_o$ in order to meet the Jacobian condition. All parameter values are normalized to their nominal values reported by Ursino et al. [1].**

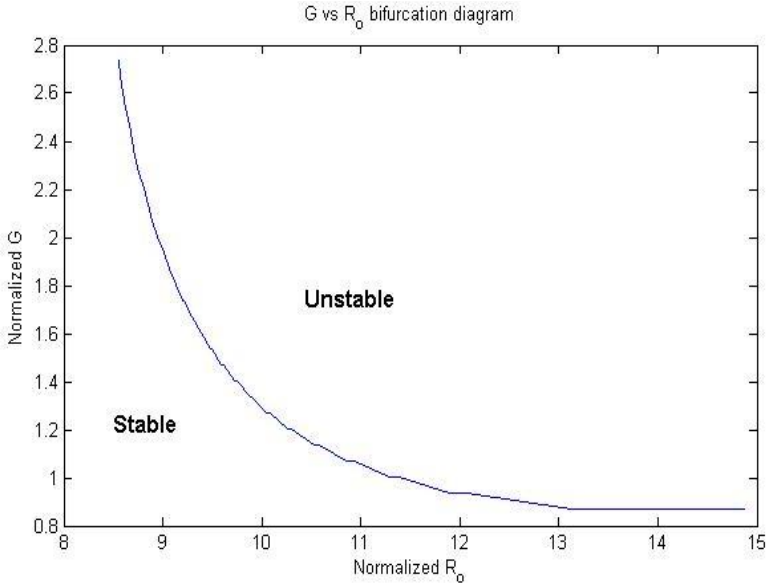


**Figure 4.4: Bifurcation diagram describing relationship between $G$ and $R_o$. The boundary of stability and instability obtained by different parameter values (gain and CSF outflow resistance) meeting the Jacobian condition mentioned in Eq (36). All parameter values are normalized to their nominal values reported by Ursino et al. [1].**

Figure 4.5 has been obtained by using different values of $K_E$ and $R_o$ combinations to see the effect of it on the eigenvalues. In order to see the effect of $K_E$ and $R_o$ , the outflow resistance was set to an almost high value (4200) and the elastance coefficient was changed from very low values to high values. The eigenvalues are shown in red and blue color. As it was expected and is shown in this figure in normal conditions when $K_E$ value is small the characteristic equations results in two negative eigenvalues that cover each other and thus only the red ones are obvious to see here. By increasing the $K_E$ value the eigenvalues start to shift to the right hand side and become complex conjugate values. At the boundary of stability and instability the real part of the eigenvalues become zero and thus at the boundary the eigenvalues are imaginary. This is exactly the combination of $K_E$ and $R_o$ that creates the bifurcation boundary. If $K_E$ is further increased the real part of eigenvalues become positive and thus unstable. It can show itself in complex eigenvalues with positive real part or positive real eigenvalues.

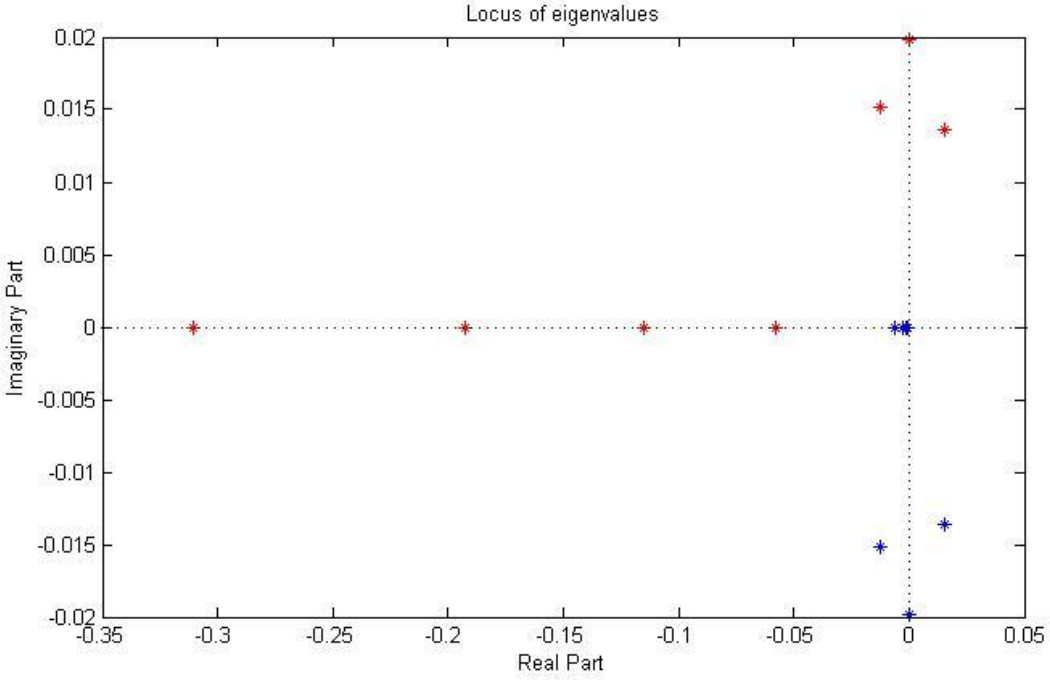


**Figure 4.5: Locus of eigenvalues. This figure shows the locus of eigenvalues (real part and imaginary part) while the values of $K_E$ and G vary from very low values to high ones. $R_o$ is kept constant in this experiment. Note that the negative eigenvalues are just the same and thus only red dots are visible in this figure.**

# Chapter 5

## 5. Sensitivity Analysis

*This chapter presents a brief description of sensitivity analysis concept at first. A preliminary study of ICP sensitivity to specific parameter variation was performed and the results of simulated ICP time pattern are presented. Finally the choice of estimation parameters based on the preliminary sensitivity study is explained briefly.*

### 5.1. Concept and background

Pressure Volume Index (PVI) test was first introduced by Marmarou et al. as a clinical procedure for deriving information regarding the intracranial pressure dynamics in patients with traumatic brain injury (TBI). The test involves injection or withdrawal of a specific amount of mock CSF (1-4 ml) to the cranial cavity in order to see how ICP is affected by this perturbation. It is assumed that the first rapid ICP response to the volume load provides information about the pressure-volume characteristic of the intracranial storage capacity, while the subsequent ICP trend reflects the status of CSF circulatory pathways [48]. Besides it's being useful for estimation of $R_o$ and CSF circulation rate, it has been recently suggested that this test can provide experts with information about the status of cerebrovascular autoregulation and cerebral hemodynamics [1].

Analysis of ICP variation during PVI tests is possible through mathematical models that include the craniospinal dynamics parameters. Different models have been suggested in order to estimate these parameters values. The first one was suggested by Marmarou et al. that could estimate the parameters values by using simple mathematical equations [19]. On the other hand the model was not complete and didn't include the effect of cerebral autoregulation and cerebral blood volume changes into account. Thus there was a need for more complete models. In these models the parameter estimation is based on the cost function minimization algorithms rather than simple analytic equations like Marmarou model.

### 5.2 Preliminary study of ICP sensitivity to parameters variation

In order to find out each parameters variation effect on the output of the model (ICP and $C_a$ prediction), a preliminary sensitivity study was performed. The model used for this aim is the same simplified model introduced in the third chapter and was implemented and simulated via Simulink library blocks in parallel with Matlab embedded functions.

The model has two state variables ICP and $C_a$, four inputs including $P_a$, $dP_a$, $P_{vs}$, $I_i$ ; where $P_a$ and $dP_a$ are a part of patient's arterial blood pressure and time derivative of that used as inputs to the model. The measurement of arterial blood pressure and intracranial pressure was performed

at Neuro-intensive Care Unit at Sahlgrenska University Hospital in Gothenburg, Sweden among patients with traumatic brain injury. ICP was monitored continuously using either a parenchymal fiber optic pressure transducer (ICP express, Codman) or a ventricular catheter (Medtronic). A Datex-Ohmeda S/5 critical care monitor collected electrocardiogram (ECG), ICP and ABP measurements at the sampling rate of 300 Hz. These signals were collected from a S/5 network, using the S5-collecting software and stored on CD-ROM [21]. ICP measurement was performed for patients with traumatic brain injury for the time interval of 1 hour for each data set. An example of ABP and time derivative of that used as input to the model are shown in Figure 5.1. As mentioned before $P_{vs}$ is set to constant value of 6 mmHg and based on absence of PVI test and CSF mock injection/withdrawal $I_i$ is set to zero.

The model consists of ten parameters including $R_o, R_f, R_{pv}, K_E, K_R, G, q_n, \tau, \Delta C_a, C_{an}$.In order to see the effect of each parameter on ICP time pattern, the parameter value was altered manually while other parameter values were kept fixed at their nominal value. The parameters that showed significant effect on ICP time pattern were $R_o, K_E, G, \tau$ and $C_{an}$. The result of this study and the analysis of the results are presented in the following sections.

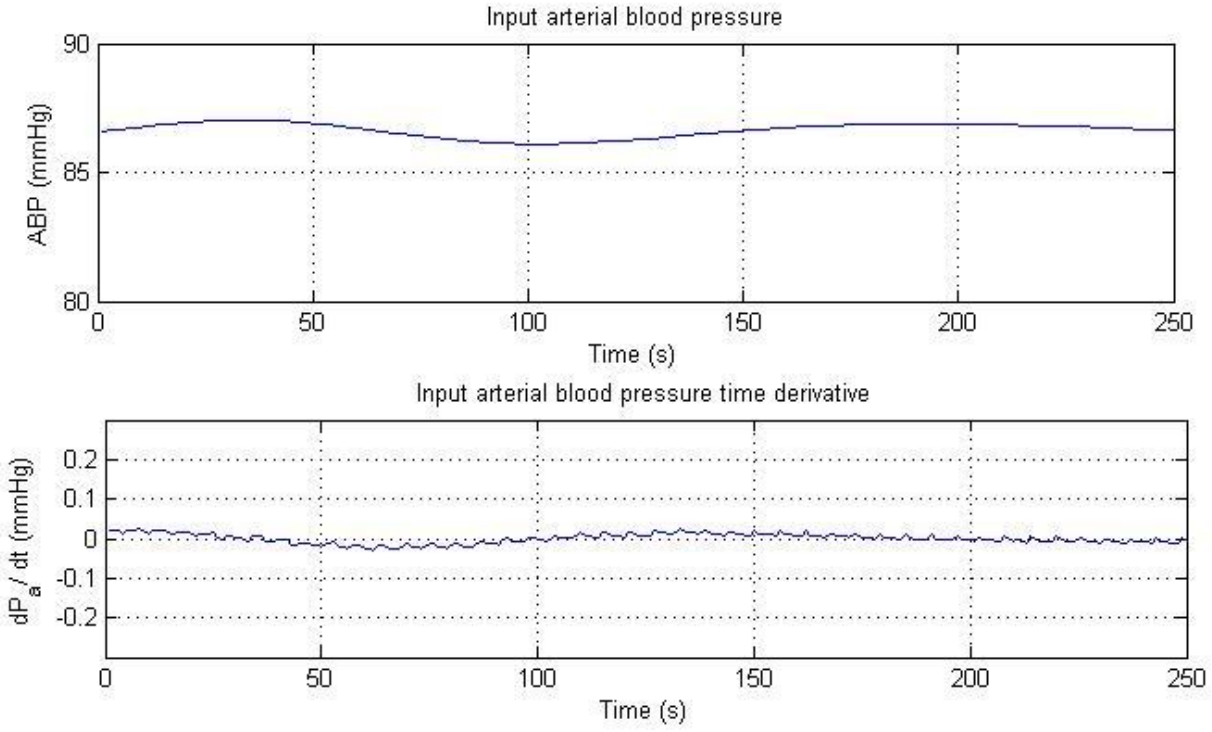


**Figure 5.1: Input to the model used for the preliminary study. The top plot is the arterial blood pressure and the bottom one is the time derivative of arterial blood pressure fed to the model for the aim of simulation of ICP time pattern.**

According to different literatures and experimental studies, CSF outflow resistance is one of the most important parameters affecting intracranial pressure dynamics. Thus it was examined in this model as well by changing $R_o$ value in a physiologically acceptable range reported by Ursino et al. and investigating the effect on ICP [1].

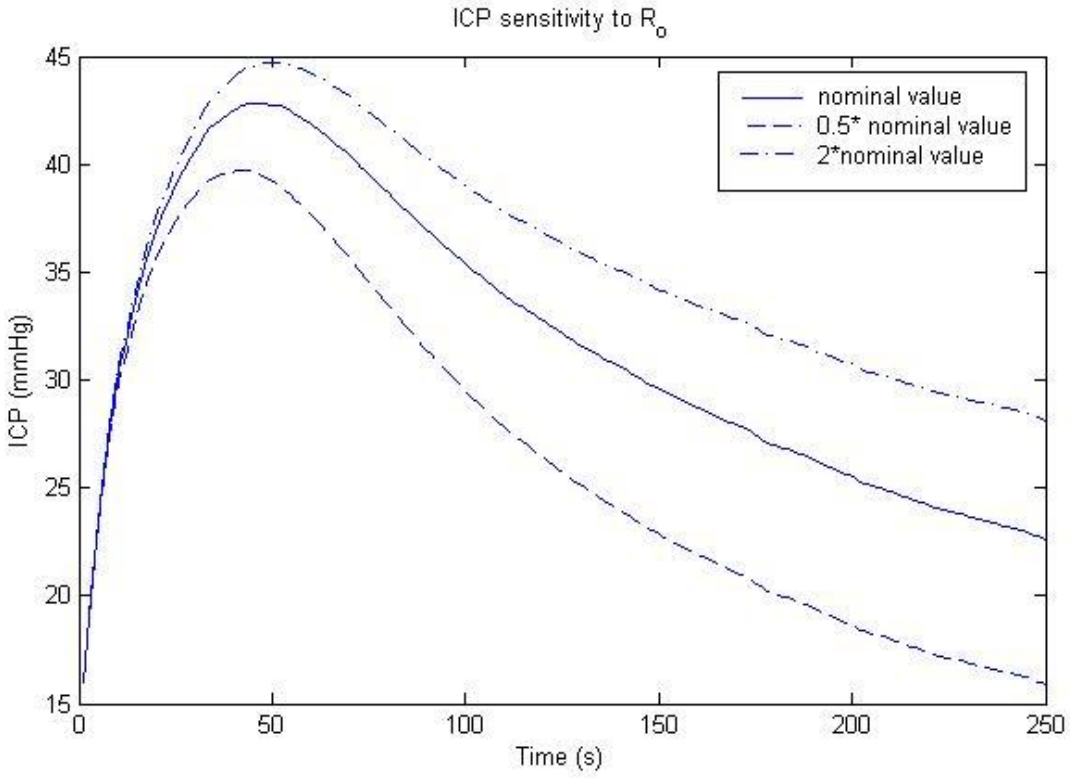


**Figure 5.2: ICP sensitivity to variation of $R_o$ value. In this process all parameters except $R_o$ are set to their nominal values. The solid curve is obtained by setting $R_o$ to its nominal value (526.3mmHg.s.$ml^{-1}$), dashed curve, ($R_o$ = 0.5$R_o$ = 263.15mmHg.s.$ml^{-1}$); dot-dashed curve ($R_o$ = 2$R_o$ = 1.0526*$10^3$mmHg.s.$ml^{-1}$)**

As obvious in Figure 5.2 the increase in CSF outflow resistance results in higher values of ICP. On the other hand it can be explained by the physiological effect of increased $R_o$ and thus less re-absorption of cerebrospinal fluid back to capillaries and resulting in increased intracranial pressure. The other feature that can be concluded from $R_o$ sensitivity analysis is that increase in Ro shifts the equilibrium level of the intracranial pressure wave upwards and vice versa.

The next parameter was $K_E$ . The procedure is the same except that this time $R_o$ is set to nominal value and $K_E$ was changed in a reasonable interval. As it can be understood from the Figure 5.3 like $R_o$ , increase in $K_E$ results in higher ICP values, this can be explained by equation 3.33 as

well that increase in the elasticity coefficient is accompanied by decrease in intracranial compliance (poor compliance) and thus higher values of ICP.

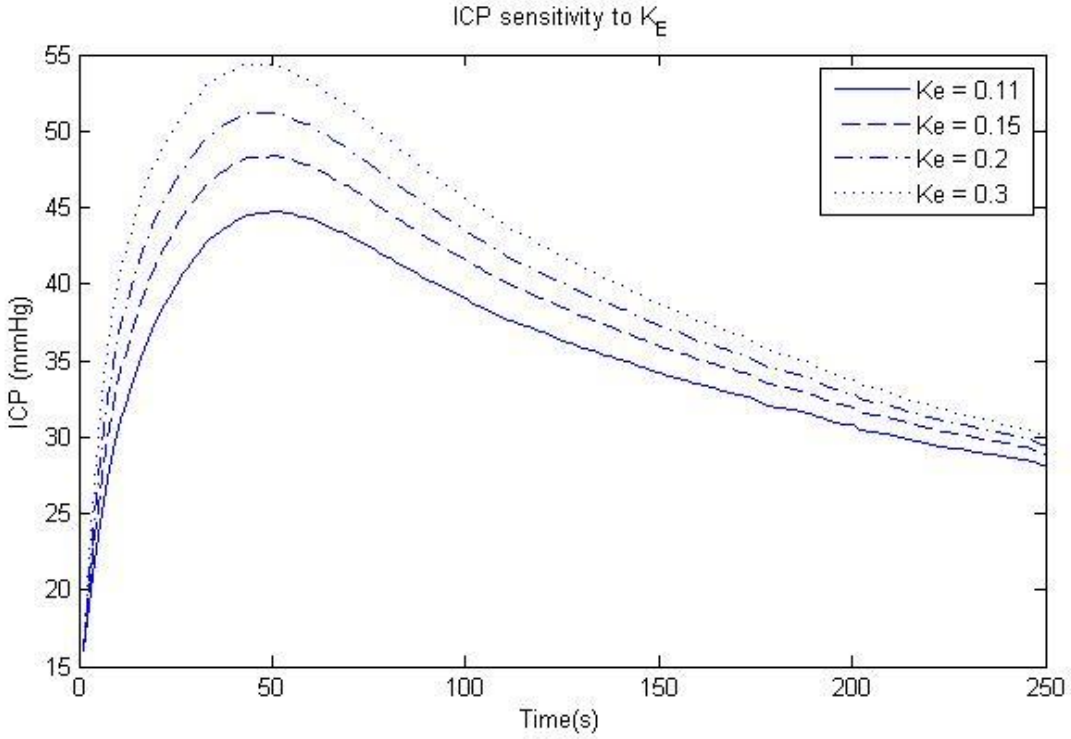


**Figure 5.3: ICP sensitivity to $K_E$variations. The solid curve, ($K_E$= nominal value = 0.11$ml^{-1}$); the dashed curve, ($K_E$=0.15$ml^{-1}$); the dot-dashed curve, ($K_E$= 0.2$ml^{-1}$); dotted curve (0.3$ml^{-1}$)**

$\tau$ (autoregulation time constant), $C_{an}$(arterial-arteriolar compliance nominal value) and G (autoregulation gain) variations showed to have significant effect on alteration of the output. Figures 5.4, 5.5 and 5.6 present the way each parameter affected the simulated ICP.

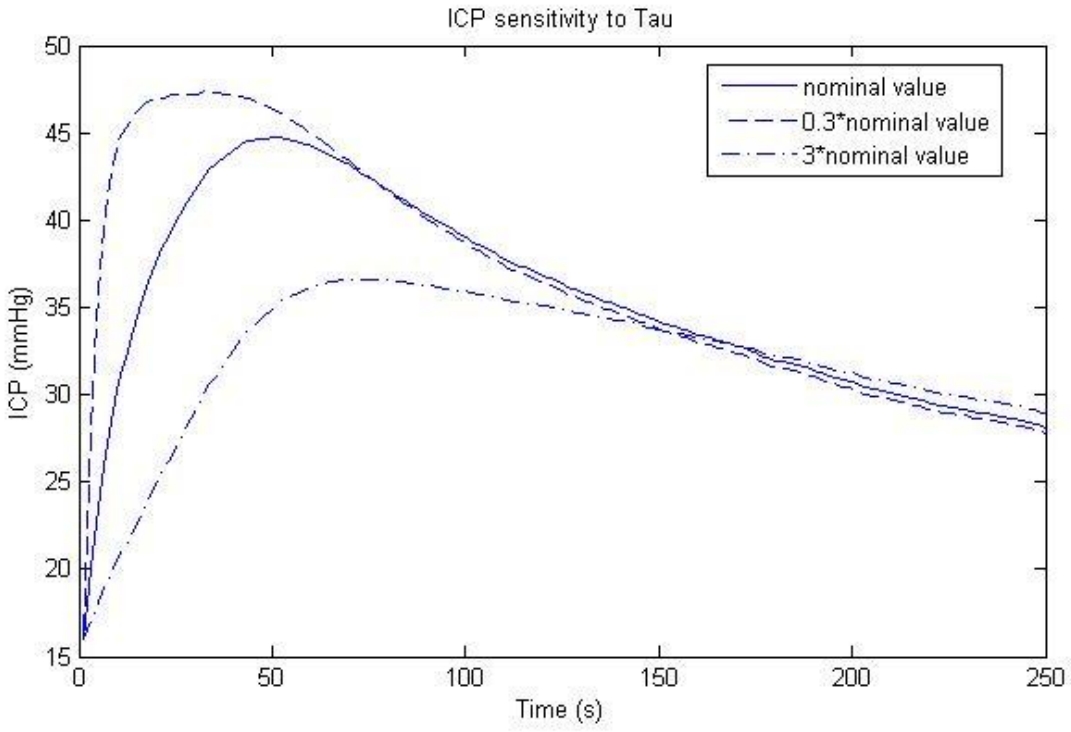


**Figure 5.4: ICP sensitivity to τ variation. The solid curve, (τ = nominal value= 20 s); the dot-dashed curve, (τ = 3*nominal value= 60 s); the dashed curve, (τ = 0.33*nominal value= 6.6 s)**

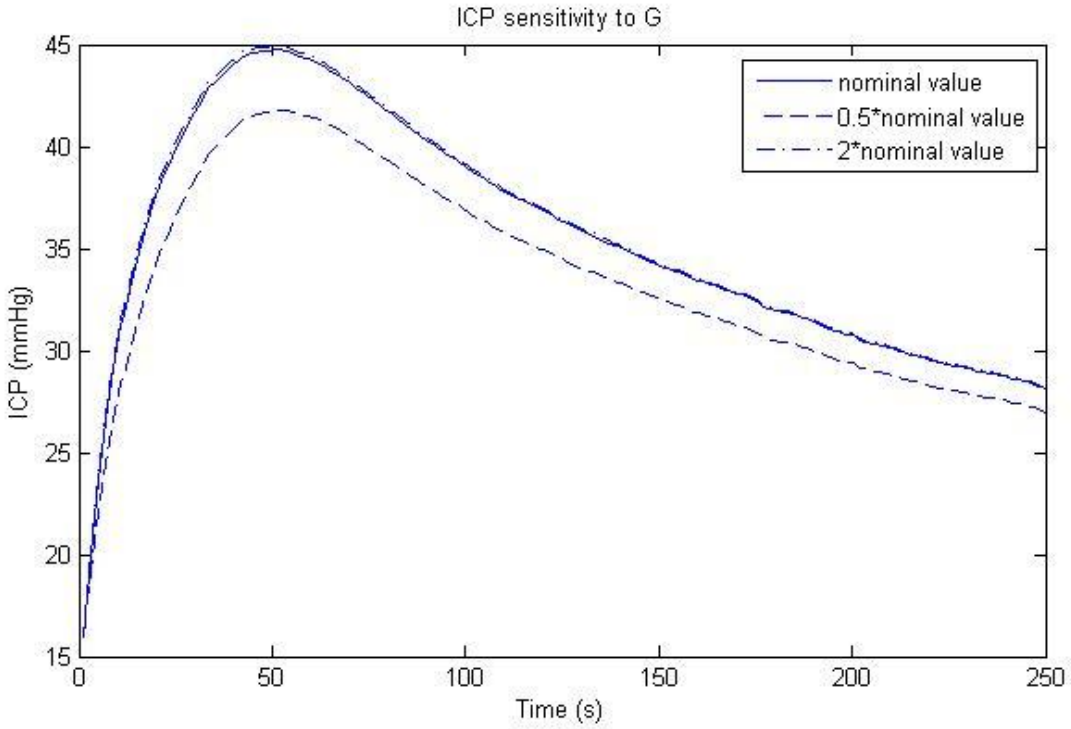


**Figure5.5: ICP sensitivity to G variations. The solid curve, (G= nominal value = 1.5ml/mmHg.100% CBF $change^{-1}$); the dashed curve, (G= 0.5* nominal value = 0.75ml/mmHg.100% CBF $change^{-1}$);and the dot-dashed one , (G= 2*nominal value = 3ml/mmHg.100% CBF $change^{-1}$); (the solid and dot-dashed curve are almost overlapping each other )**

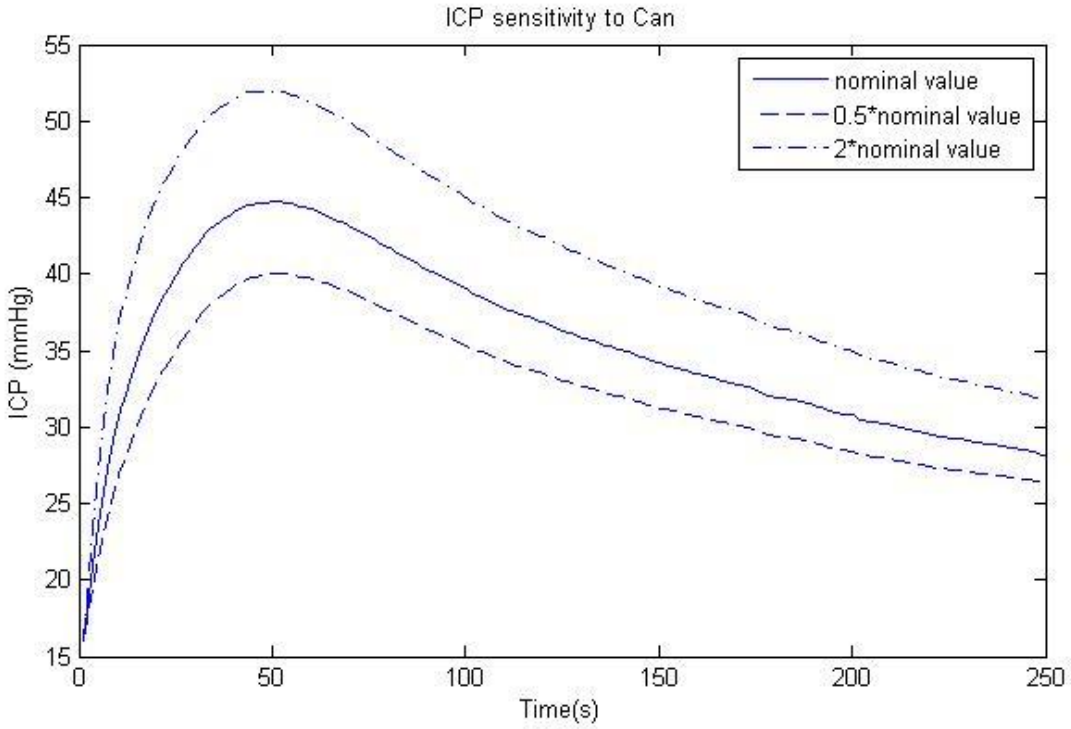


**Figure 5.6: ICP sensitivity to $C_{an}$ variation. The solid curve ($C_{an}$= nominal value = 0.15ml/mmHg); the dashed curve, ($C_{an}$= 0.5*nominal value = 0.075ml/mmHg); the dot-dashed curve, ($C_{an}$= 2*nominal value = 0.3ml/mmHg)**

Other parameters variations didn't show that much effect on the intracranial pressure dynamics or some minor alteration was observed but since it was neutralized by the other parameters variation, there was no need for considering them as significant parameters affecting intracranial dynamics. In the next section the parameter choice for estimation and the reason behind each choice is described more in details.

## 5.3 Choice of Estimation parameters

One of the important problems that needs to be solved while working with an optimization/minimization algorithm is first to choose the parameters to be optimized/estimated. This model consists of the following parameters:

- CSF formation and absorption resistance ($R_o$ , $R_f$)
- Intracranial elastance coefficient ($K_E$)
- Central autoregulation gain (G)
- Autoregulation time constant ($\tau$)
- Amplitude of sigmoidal autoregulation characteristic (saturation level) ($\Delta C_a$)

- Nominal value for the arterial compliance ($C_{an}$)
- Nominal value for the cerebral fluid flow ($q_n$)
- Resistance of the large cerebral veins ($R_{pv}$)
- Initial values for the states ($C_a(0), P_{ic}(0)$)

As it was mentioned before there is a need for some model parameters to be chosen as priori to be modified during the optimization algorithm. The algorithm is based on minimization of the difference between the model prediction and the clinical recorded data. A cost function is defined for this aim which will be more explained in the next section. The identification of these model parameters to be estimated is based on

1) Acceptable fit between the real data and the model predictions
2) Accuracy of parameter estimations
3) The physiological and clinical relevance of the estimates

In order to find out which parameters are most likely to affect the dynamics of model predictions, as described in the previous section, some simulations were examined manually with changing the parameter values in a reasonable range during each simulation while having all other parameters fixed at their nominal values. In addition to finding important parameters to be estimated, this study provided us with a practical knowledge about in what ways each parameter might affect the output of the model and this was also compared and analyzed by using both model equations and also different clinical situations leading to the same results.

This study suggested that venous resistance doesn't have a crucial role on ICP during the simulations. As suggested by Ursino group only the $R_o$ /$R_f$ could be identified with good accuracy [1, 32]. Thus the $R_f$ and $R_{pv}$ values were set to their nominal values and only $R_o$ was chosen to be changed during the minimization algorithm. Since during the study only the central slope of autoregulation characteristic (G) was changing according to the minor variation in CPP but not the saturation level, the CBF nominal value $q_n$ and $\Delta C_a$ were set at their nominal values.

Accordingly the parameters chosen to be used in the minimization algorithm were $R_o$, $K_E$ , G and $\tau$. These parameters proved to show different aspects of intracranial dynamics. Although these parameters seemed to be sufficient for the optimization algorithm but according to some model limitations in some cases there is a need for additional parameters to be introduced in order to obtain good fit between model prediction and real data. For example the nominal value of arterial-arteriolar compliance and amplitude of sigmoidal autoregulation characteristics ( $C_{an}, \Delta C_a$) were added to the estimation parameters vector in order to have an accurate reproduction of ICP. The following chapter is mostly devoted to explanation of minimization algorithm, mathematical procedure and some important statistical equations that are needed for validation of model afterward. The results of estimated versus real ICP and correlation between parameters are also presented.

# Chapter 6

## 6. Sensitivity analysis results

*As described in the previous chapter the aim of sensitivity analysis is to find out how each parameter variation can affect the output of the model. One way to look at parameters is the mathematical point of view in which each parameter's effect can be described according to the model's equations. On the other hand these parameters represent different clinical/physiological aspects of patients' situation. Thus a deep understanding of each parameter and its alteration effect on ICP is of great importance.*

*In this chapter after a short description of the concept of cost function, parameter estimation, minimization algorithm and parameter sensitivity, the results obtained from the automatic parameter estimation are brought and explained briefly. A comparison between models prediction and experimental data has been done to see how effectively the model has predicted the intracranial pressure. Finally the results obtained from analysis of correlation between parameters are presented and analyzed.*

### 6.1 Cost function, Parameter Estimation and minimization algorithm

The aim of this study is to first find the best fit between the model and experimental results by tuning a set of estimation parameters in a way to minimize the difference between real and simulated ICP time pattern. The second goal of this study is to find the effect of each parameter on ICP variation in order to have a deeper grasp of what mechanisms are most likely to influence the ICP in the model and how these mechanisms interact with each other.

As mentioned in equation 4.15, the model consists of ten parameters. For the simplification of the study, some of these parameters are chosen to be the main ones affecting the craniospinal system dynamics and can be selected to be estimated through an iterative automatic optimization algorithm (see section 5.3 for better understanding of choice of estimation parameters). The optimization algorithm starts by an initial guess set by the user and tries to find the optimum parameter values iteratively by looking for the values in a suitable range that lead to the best fit between the measured/real data and the result of model predictions.

Since the estimation procedure is based on minimizing the difference between the model's prediction and the experimental data (cost function), one of the suitable approaches that can be used for this aim is using the least square cost function. Thus the algorithm aims to minimize the cost function $F(\theta)$ defined by

$$F(\theta) = \sum_{i=1}^{N} \left[ P_{ic}^{(s)}(t_i) - P_{ic}^{(m)}\left(t_i, P_a(t_i), \dot{P}_a(t_i), I_i, \theta\right) \right]^2 \qquad (5.1)$$

Where $P_{ic}^{(s)}(t_i)$ is the filtered experimental ICP value at the time instant $t_i$ and $P_{ic}^{(m)}(t_i)$ is the model prediction for ICP at the same time, $P_a(t_i)$ is the arterial blood pressure, $\dot{P}_a(t_i)$ stands for the arterial blood pressure time derivative, $I_i$ is the injection rate which is neglected for this application due to clinical limitations and finally the parameter values $\theta$. The parameters that are used in this minimization algorithm are the same ones as described in the previous section plus the initial value of model states.

The job of the minimization algorithm is thus to change the values of defined parameters in a way to minimize the cost function. There are different ways to implement the minimization algorithm. One way could be to use the optimization toolbox of Matlab and introduce the Simulink model as a function whose parameters need to be optimized. This study took advantage of the Parameter Estimation toolbox as a new feature introduced by Matlab R2008. One advantage of using this toolbox instead of the optimization toolbox is that in the parameter estimation toolbox there would be no need for introducing a cost function separately. Another good feature about this toolbox is that there is a chance of choosing among different methods such as nonlinear least square, Gradient, Pattern search or Simplex methods that might suit the specific application.

The estimation options should be chosen in a way to estimate the mentioned parameters in a reasonable range that can be defined manually by maximum and minimum values for each parameter. Defining suitable values for initial guess, maximum and minimum values for parameters has an important effect on improving the estimation results. On the other hand since this model might be fed afterwards with different patients' experimental data, there should be a way to adjust the initial values of the states (ICP and $C_a$) so that the estimation starts from a better guess. This can be done by setting the initial state values as two of the parameters to be estimated as well. Thus while changing the input data from one patient to another patient the initial state values are optimized automatically according to the characteristics of the input data. In other words using some prior knowledge of patients' clinical situation could be useful for both speeding up the estimation procedure and also omitting the risk of having unexpected parameter values. Once all estimation parameters and options are set, the minimization algorithm can be run to find the best fit between the introduced ICP reference data and the simulated one predicted by the model.

## 6.2 Parameter sensitivity

In order to understand each parameter alteration effect on the output of the model (ICP), the sensitivity matrix can be defined and computed by

$$S(t) = \left[\frac{\partial P_{ic}^{(m)}(t_i, P_a(t_i), \dot{P_a}(t_i), I_i, \theta)}{\partial \theta}\right]_{\theta=\hat{\theta}} \quad (5.2)$$

where $P_{ic}^{(m)}\left(t_i, P_a(t_i), \dot{P}_a(t_i), I_i, \theta\right)$ is the model's prediction of ICP at the time instant $t_i$. In other words parameter sensitivity shows how big each parameter variation affects the error of models prediction. Thus assuming the difference of model's prediction and recorded ICP as estimation error the previous equation can be re-written like

$$S = \left[\frac{\partial E}{\partial \theta}\right]_{\theta=\hat{\theta}} \quad (5.3)$$

where E represents the estimation error at the parameter value of $\theta = \hat{\theta}$.

The following sections present the preprocessing/filtering phase performed to prepare the data needed to be used as input in the estimation algorithm. The Results of the parameter estimation and cost function minimization, figures of measured versus simulated data and parameter correlations are presented as well.

## 6.3 Filtering and preprocessing the clinical data

The model introduced by Ursino et.al is only able to reproduce low frequency components of ICP [1]. Accordingly this model is not able to trace pulsating changes produced by sphygmic wave or respiration. Thus all experimental data (ABP, its time derivative and reference ICP) need to be filtered first and then fed to the estimation software as inputs/outputs.

First the data needs to be down-sampled since the sampling frequency of 300 Hz seems to be really high for this application. This can be done by using different functions such as 'down sample' in Matlab, but since the aim of this part was to filter and down sample the clinical data the 'decimate' function can be used as well. The Sphygmic wave can be eliminated by using a low-pass Finite Impulse Response (FIR) filter with 128 coefficients and the cutoff frequency of 1 Hz using the Hamming window technique as suggested by Ursino group [48]. This will omit the high frequency components of both ABP and ICP. After this the respiratory pulsation can be omitted using a moving average FIR filter in order to smooth the arterial and intracranial waves.

The down sampled filtered data is then used in the parameter estimation procedure as input data (ABP and d$P_a$/dt) and the ICP will be used as the output data that the model prediction is supposed to fit with.

Figure 6.1 shows the raw arterial blood pressure recorded at hospital, the second plot presents the raw data (ABP) recorded at hospital, the down-sampled and finally the filtered and down-sampled ABP after removing sphygmic and respiratory pulsations.

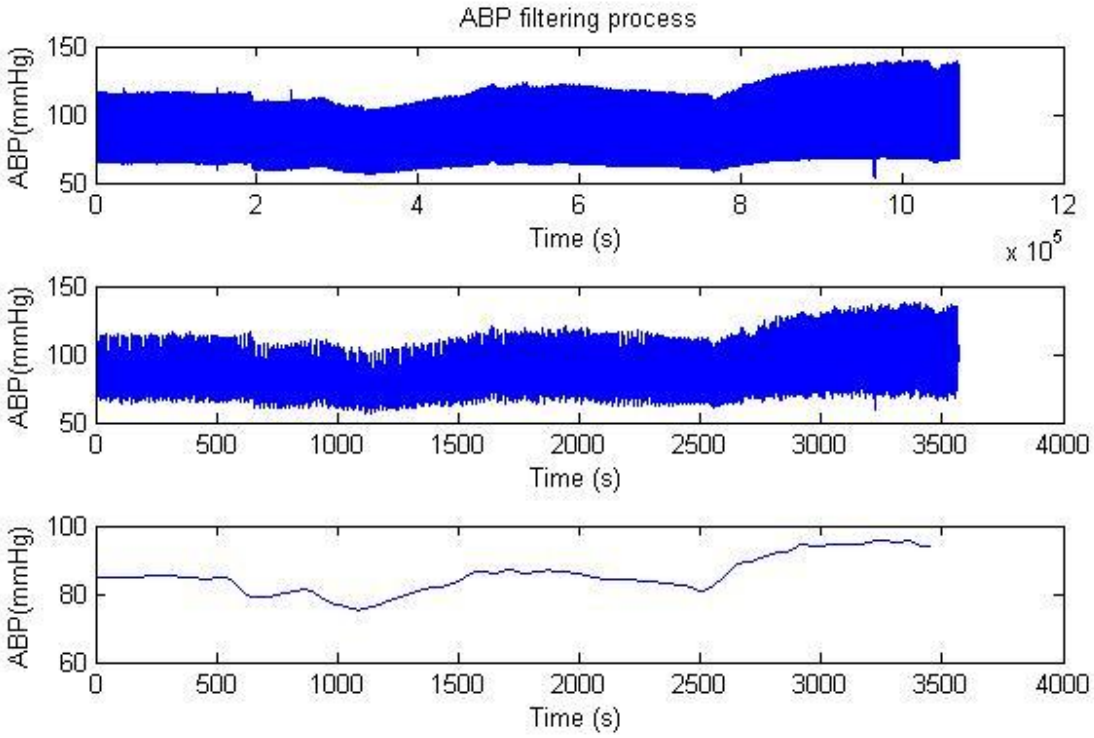


**Figure 6.1: Filtering and down-sampling clinical data. This figure represents the preprocessing phase of the experiment including the real raw data (top), the data is down-sampled (middle ) and sphygmic wave and the respiratory pulsations are filtered as well (bottom).**

Although the data is filtered, but there might still exist some outliers according to sudden changes in patients' situation which result in wrong parameter estimation far away from what was expected according to clinical prior knowledge of patient's situation. A possible way to improve the estimation procedure results is to preprocess the data for estimation. Since the model is not able to reproduce the picks or sudden changes, the outliers should be removed from both input and reference output. The possibility to exclude (directly or graphically) a range of unwanted data from the estimation input or ICP and also the facility of handling missing data are other features that might be useful in improving estimation results while manipulating with noisy or unstable inputs.

## 6.4Parameter Estimation Results

After setting which parameters are needed to be estimated and set those parameters to their initial values, adjusting reasonable ranges for maximum and minimum parameter values, correcting parameter and function tolerance level if needed, setting the number of iterations for estimation process and finally feeding the software with the filtered and preprocessed data, the software is ready to estimate the parameter values leading to best fit with the experimental ICP.

As mentioned before except the estimation parameters the other parameters are set to their nominal values. The nominal values used for all parameters except the ones that are estimated are the ones presented in table 6.1. After estimation is done the optimum parameter values that lead to minimum cost function are saved and presented in table 6.2. All values are normalized with respect to their nominal values in order to make it easier to compare and evaluate them.

**Table 6.1: Values for the model parameters, input quantities, pressures and state variables**

| **Nominal values for Model parameters** | |
|---|---|
| Parameter | Value |
| $R_o$ | 526.3 mmHg.s.$ml^{-1}$ |
| $R_{pv}$ | 1.24 mmHg.s.$ml^{-1}$ |
| $R_f$ | 2.38× $10^3$mmHg.s.$ml^{-1}$ |
| $\Delta C_{a1}$ | 0.75 ml/mmHg |
| $\Delta C_{a2}$ | 0.075 ml/mmHg |
| $C_{an}$ | 0.15 ml/mmHg |
| $K_E$ | 0.11 $ml^{-1}$ |
| $K_R$ | 4.91× $10^4$ mmHg$^3$.s.$ml^{-1}$ |
| τ | 20 s |
| $q_n$ | 12.5 ml/s |
| G | 1.5 ml.mmHg$^{-1}$. 100% CBF change$^{-1}$ |
| **Input quantities , pressure, and state variables in nominal conditions** | |
| $P_a$ | 100 mmHg |
| $P_{ic}$ | 9.5 mmHg |
| $P_c$ | 25 mmHg |
| $P_{vs}$ | 6.0 mmHg |
| $C_a$ | 0.15 ml/mmHg |

$R_o$ represents the CSF outflow resistance; $R_{pv}$ , proximal venous resistance; $R_f$, cerebrospinal fluid formation resistance; $\Delta C_{a1}$ , and $\Delta C_{a2}$ , amplitude of sigmoidal curve; $C_{an}$ ,nominal value of arterial compliance; $K_{E,}$ , elastance coefficient; $K_R$, resistance coefficient; τ , time constant; $q_n$, nominal value of cerebrospinal fluid; G , gain; $P_a$ ,systematic arterial blood pressure; $P_{ic}$, intracranial pressure; $P_c$, capillary pressure; $P_{vs}$ , dural sinus pressure; $C_a$ , arterial compliance[1].

Table 6.2 suggests that in case of high ICP values $K_E$ is mostly increased, which shows the poor intracranial compliance according to equation (3.33). The values match with the range reported by different clinical literatures for patients with various intracranial diseases [48, 49, 50].

**Table 6.2: Estimated parameter values**

| **Estimated parameter values normalized over the nominal values** | | | | | | |
|---|---|---|---|---|---|---|
| Case | $R_o/R_{o0}$ | $K_E/K_{E0}$ | $G/G_0$ | $\tau/\tau_0$ | $C_{an}/C_{an0}$ | $\Delta C_{an}/\Delta C_{an0}$ |
| #1 | 3.218 | 0.124 | 0.256 | 3.345 | - | - |
| #2 | 18.123 | 0.828 | 1.997 | 5 | 0.371 | 0.345 |
| #3 | 4.871 | 0.0827 | 0.203 | 4.9996 | - | - |

Represents the results of parameter values gained by estimation algorithm. $R_o$ represents the CSF outflow resistance; $K_E$ , elastance coefficient; G, gain and $\tau$ is the time constant. The index zero represents the nominal value for each parameter. The values are normalized in order to make the comparison easier. In case #2 there was a need for extra parameter to be estimated $\frac{\Delta C_a}{\Delta C_{a0}} = 0.345$ , $\frac{C_{an}}{C_{an0}} = 0.371$ in order to obtain a reliable result.

$R_o$ is also increased for patients with high ICP values. This agrees with the discussions brought in the stability analysis where high values of $K_E$ and $R_o$ lead to unstable ICP output. The greater value of Ro represents less CSF absorption or poor CSF circulation which consequently results in higher values of ICP. G and $\tau$ show different behaviors for various patients. In patients with good autoregulation the value for G should be close to the nominal value or higher since G represents the autoregulation gain and effective autoregulation means higher values for G, and the autoregulation time constant $\tau$ should be low. When the patient has weak or slow autoregulation or is in sever level of TBI the G value will decrease and $\tau$ increases instead.

The top plot in Figure 6.2 is the presentation of arterial blood pressure which was used as the input to the parameter estimation algorithm to simulate an ICP which fits the best with the recorded one. As it can be understood from the bottom plot of Figure 6.2, the gray curve represents the real ICP which was measured at the hospital and the blue one is the result of estimation process. In other words the parameters have been set in a way to minimize the difference between these two curves. The measured versus simulated ICP shows a satisfactory agreement between the measured data (recorded at hospital) and the simulated one.

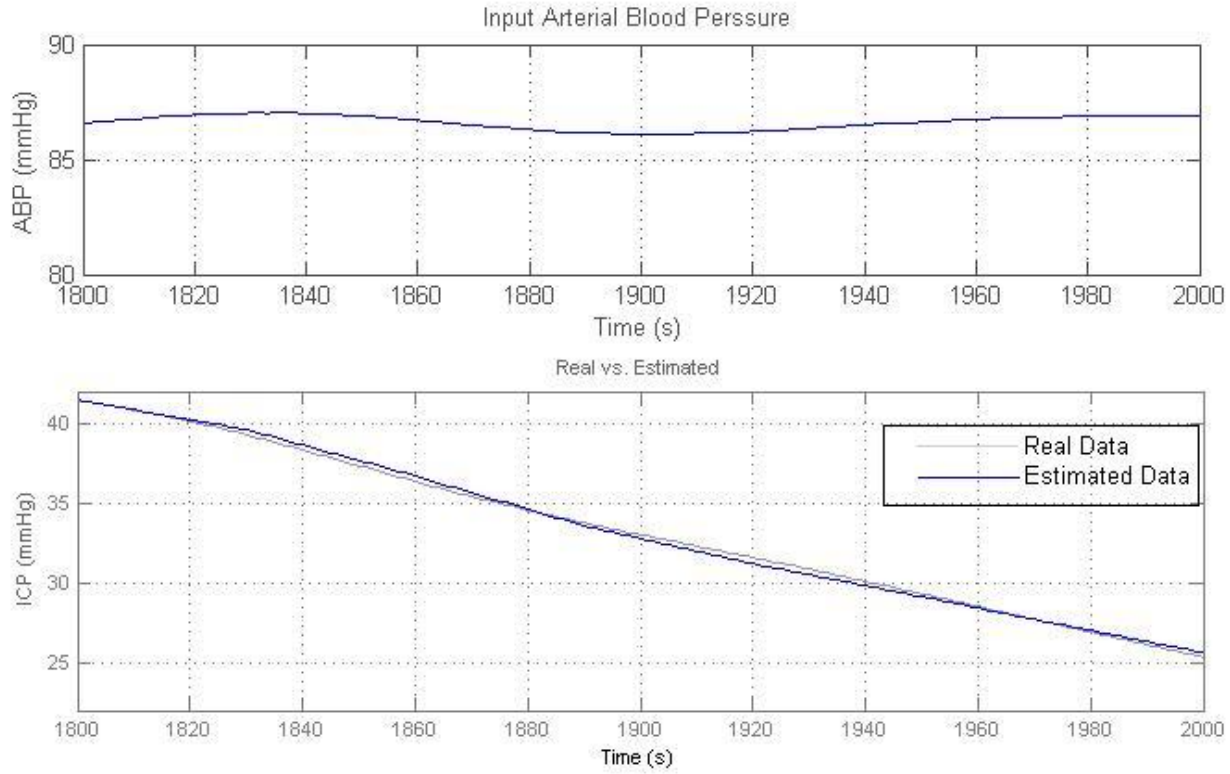


**Figure 6.2: ABP and Real versus estimated data case #1. Upper plot represents the real arterial blood pressure used as the input, the bottom part is the presentation of real data (gray line) versus the simulated one (blue line) via the estimation algorithm.**

Figures 6.3 and 6.4 show the ABP and equivalent measured versus simulated ICP respectively for two other cases.

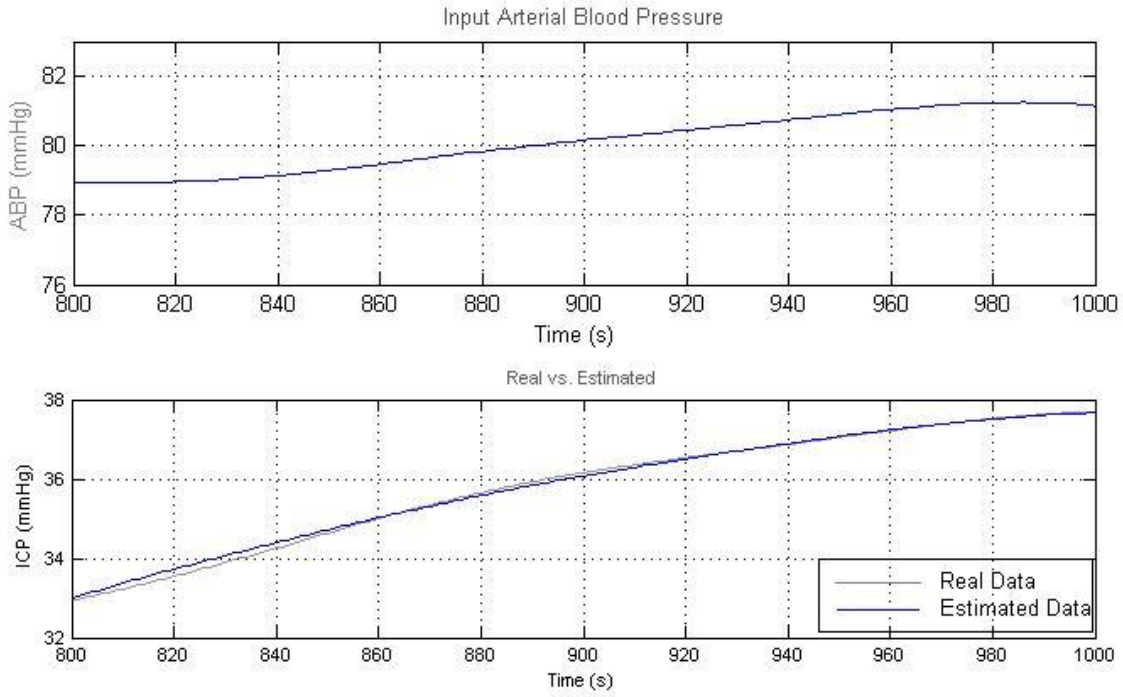


**Figure 6.3: ABP and Real versus estimated data case #2. Upper plot represents the real arterial blood pressure used as the input, the bottom part is the presentation of real data (gray line) versus the simulated one (blue line) via the estimation algorithm.**

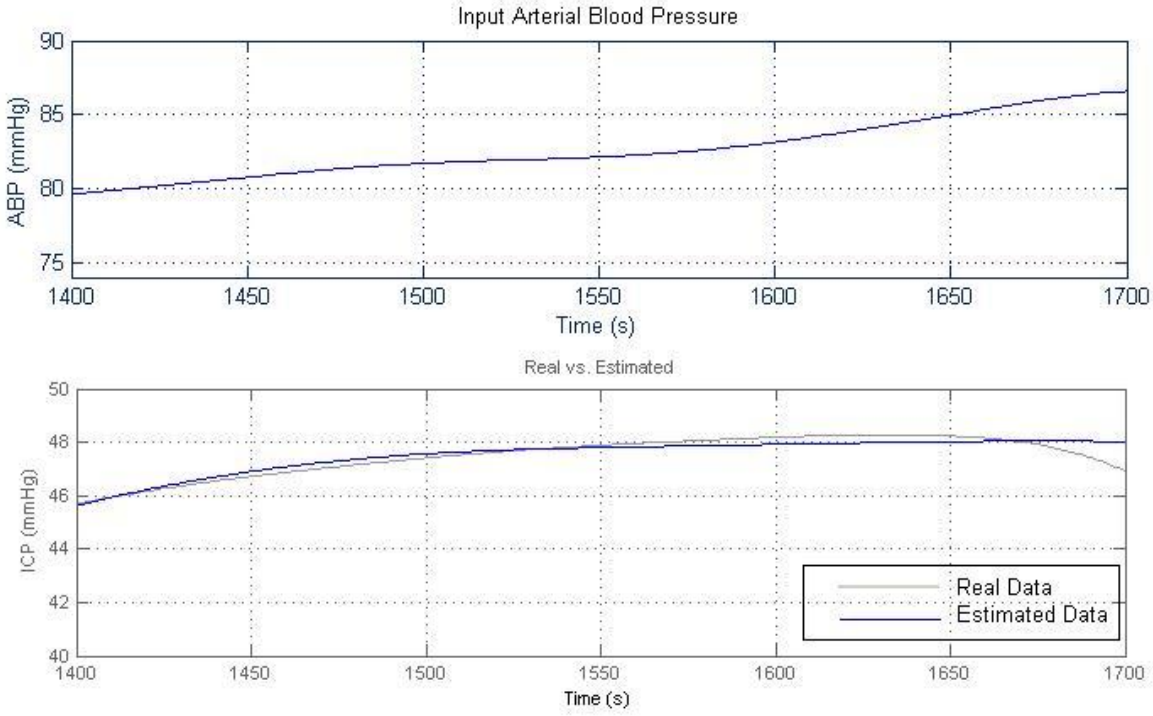


**Figure 6.4: ABP and Real versus estimated data case #3. Upper plot represents the real arterial blood pressure used as the input, the bottom part is the presentation of real data (gray line) versus the simulated one (blue line) via the estimation algorithm.**

Cost function as described before is a presentation of the difference between the real data and simulated one and depending on the number of iterations set for the optimization algorithm, initial values of the states and parameters to be estimated, method used to find the optimum values for parameters (nonlinear square error, pattern search, Genetic algorithm, etc) and other estimation options can vary significantly. Figure 6.5 shows the cost function obtained from optimization algorithm responding to case #2 presented in Figure 6.3.

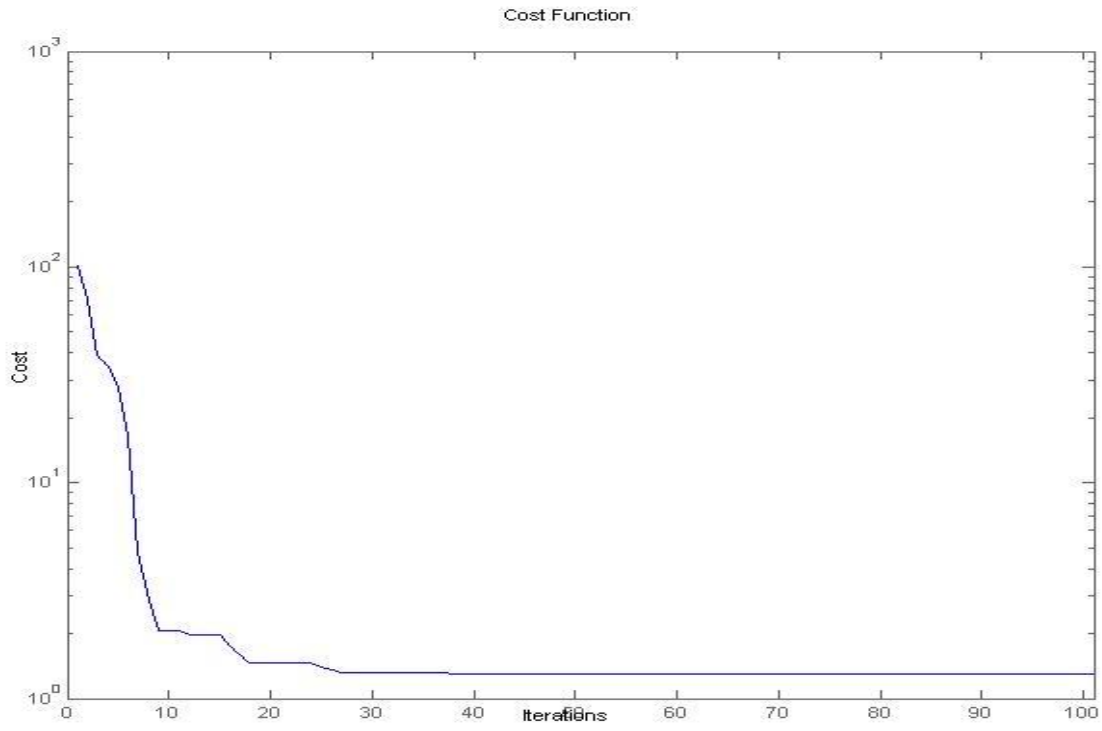


**Figure 6.5: Cost function diagram. This figure shows the values for the mentioned cost function in the iterative parameter estimation process. As expected the value of cost function decreases as the algorithm tries to find the best fit for the parameter values. The lookup for the best fit continues until one of the conditions/options set initially for the software is met.**

As it can be understood from the figure the cost function might start from a high value but the algorithm changes the parameters in a way to reduce the cost function as far as it meets the optimization options. The less cost function is, the closer the real data and the simulated one would be. It is worth to mention that since the model was not designed to simulate sudden peaks and changes in ICP, if the input ABP has sudden alterations the cost function would increase. This agrees with the results suggested by Ursino et al. [48]. They also concluded that the model was not able to estimate the sudden variations caused by PVI maneuver during bolus injection or withdrawal.

## 6.5Parameter sensitivity and correlation between parameters

As explained before one of the main aims of sensitivity analysis is to evaluate the way each parameter affects the ICP time pattern. The preliminary study somehow showed the effect of each parameter on ICP. Another good feature that can be studied and is of high clinical value is to study the correlation between each two estimation parameters. The value of this study is in understanding how each two set of parameters effect on ICP and what is the correlation between them. In other words, by studying the correlation between parameters one can understand how one parameter variation can be compensated or amplified by the other parameter.

To better understand the meaning of studying the correlation between estimation parameters lets first concentrate on analytical description of this correlation. As mentioned before the aim of optimization (parameter estimation) algorithm was to estimate the value of estimation parameters in a way to minimize the cost function and thus to produce a better fit between models prediction and the real measured data. A question that arises while estimating parameters values is that how much each estimation parameter can vary in a way that the cost function remains the same. In other words, when estimating parameters every two set of the parameters are allowed to vary in a specific interval in a way that ICP and cost function don't change. This idea was first suggested by Ursino et al. [48] when a so-called ∈-Indifference region was produced by varying parameters in a way that the difference between the new cost function and the previous one is less than ∈.

$$|F(\theta) - F(\hat{\theta})| < \in \qquad (6.1)$$

Where $\theta$ is the parameter value in a non-optimal situation and $\hat{\theta}$ is the optimal value of parameter $\theta$. Thus the equation simply is defined to find the parameters that produce a cost function $F(\theta)$ where the change from the optimal cost function $F(\hat{\theta})$ is less than ∈. In other words how much one can change the parameter value with respect to its optimal value in a way that the cost function variation is not noticeable. The set of parameter values that meet these equations are called ∈-indifference region. A good advantage of studying the correlation between parameters is that it helps us to understand which parameters are the most significant ones in affecting on ICP and which ones are not. Its worth to mention that the ellipses obtained from parameter correlations are local to the optimal value and would vary from one patient to another both in shape, center and direction.

After the optimum values of parameters were obtained from the estimation algorithm, a simple function can be written to find the parameter values that meet equation (6.1). The correlations between each two estimation parameters in case #2 are presented in Figures 6.7.

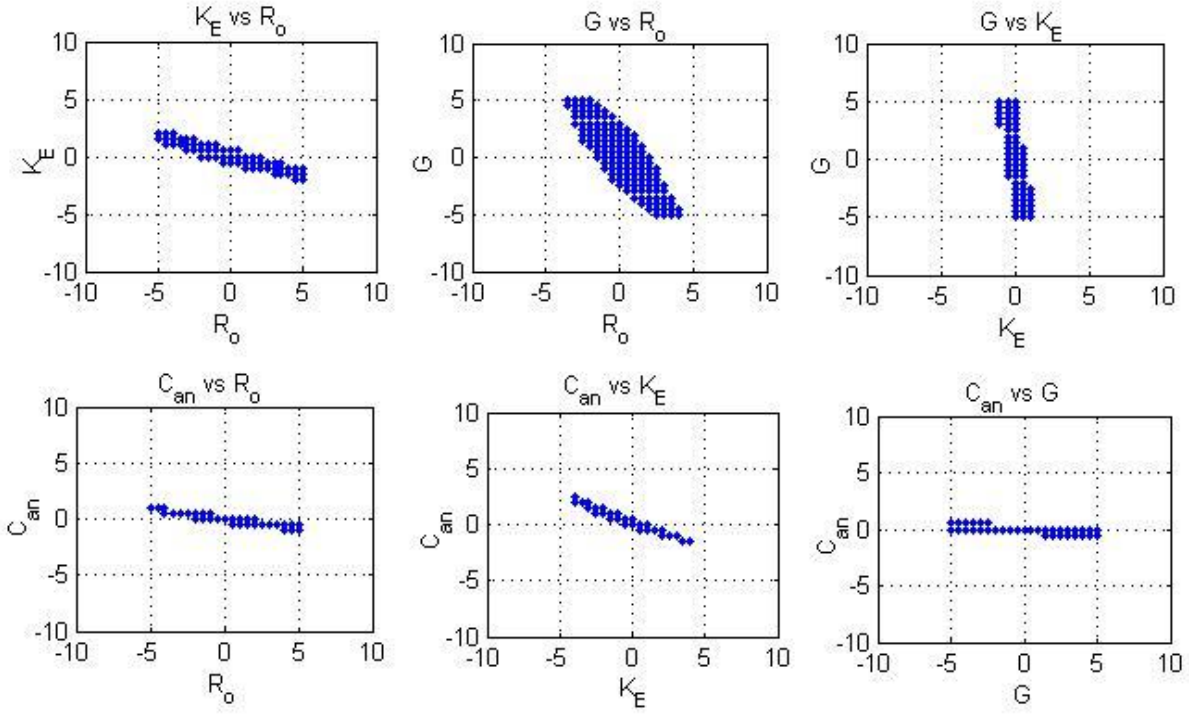


**Figure 6.6: Parameters correlations . 5%Indifference regions for showing the correlation between every two parameters for case #2. The ∈ value was set to 0.05. The top left shows the correlation between elastance coefficient ($K_E$) and CSF absorption resistance ( $R_o$). The top middle is autoregulation gain (G) correlation with CSF outflow resistance ($R_o$). The top right is the autoregulation gain (G) versus ($K_E$) correlation. The bottom raw presents correlation between arterial-arteriolar compliance nominal value and CSF absorption resistance $R_o$(bottom left), elastance coefficient $K_E$(bottom middle) and autoregulation gain G (bottom right).**

### 6.5.1 Correlation between $K_E$ and $R_o$

As it can be understood from Figure 6.7 $\mathbf{K_E}$ and $\mathbf{R_o}$ parameters are showing negative correlation since the produced region, which looks like an ellipse, is located in the second and fourth quadrants. When both parameters change in the same direction (shorter axis) the ICP is significantly affected but when these parameters vary in the opposite direction (longer axis) the ICP is scarcely affected. This is understood by looking at the longest and shortest axes of the produced ellipse. While longest axis shows that by changing that parameter in a wide range ICP and cost function are not significantly affected, the shorter axis shows that even a small variation of that parameter causes ICP and cost function to vary. Thus from this figure we understand that first the correlation between the two parameters is negative or in other words the increase in one parameter can be compensated by decrease in the other one. At last the bigger the ratio of longest axis to the shortest axis is the more closely the two parameters are. Thus $K_E$ and Ro are very closely correlated as shown in Figure 6.7.

### 6.5.2 Correlation between G and $R_o$

Again it can be recognized that G and $R_o$ are showing negative correlation while $R_o$ variation again seems to have less effect on ICP and cost function comparing to G . ICP is only scarcely affected if the parameters vary in the direction of longer axis (opposite direction) and more significantly affected if parameters vary in the direction of shortest axis (same direction). In other words when gain is increased CBF would increase and capillary pressure and thus CSF production rate would increase as the result. This can be compensated by decrease in $R_o$ value which is exactly what the correlation Figure 6.7 suggests. Comparing this figure with previous one, we can see that the ration of the longer axis to the shorter one is decreased and thus G and Ro are less correlated in comparison with $R_o$ and $K_E$.

### 6.5.3 Correlation between G and $K_E$

G and $K_E$ show an inverse correlation. Increase in G results in increase in ICP value which can be compensated by decreasing $K_E$ or in other words improving intracranial compliance ($C_{ic}$). Again the longer axis ratio to the shorter one is big and thus these two parameters are very closely correlated.

### 6.5.4 Correlation between $C_{an}$ and $R_o$

A good feature of studying the correlation between estimation parameters was that we understood that in some cases inclusion of estimation of arterial blood volume changes ($C_{an}$) was beneficial in obtaining a good fit between measured and simulated data. In other words including the effect of $C_{an}$on ICP for estimation purpose led to better results for cost function and measure versus simulated data fit. Figure 6.7 illustrates a negative correlation between $R_o$ and $C_{an}$. The ellipse is very close to a horizontal one which shows a very high ratio of longer to shorter axis and thus these parameters are very closely correlated.

### 6.5.5 Correlation between $C_{an}$ , $K_E$ and G

Figure 6.7 shows that $C_{an}$ and $K_E$, are negatively correlated again. The same thing happens while studying the correlation between $C_{an}$ and G. The parameters show an almost negative correlation with a big longer to shorter axis ratio. The high $C_{an}$values can be compensated by increasing the CSF outflow (reduction of $R_o$), improvement of intracranial compliance (reduction of $K_E$) and/or reduction of autoregulation gain (G). The results obtained from this study show a satisfactory agreement with the ones suggested by Ursino et al. [48].

# Chapter 7

## 7. Discussion and future work

*This chapter aims to give a brief discussion of the major findings of this study and the meaning of the obtained results. It also includes mentioning some of the main limitations faced with while performing this research. Finally some suggestions are offered for the aim of possible future work in the relevant area.*

### 7.1 Discussion

The main contribution of this work was to describe the interrelationship between cerebral hemodynamics and intracranial pressure by using a simple mathematical model. The stability analysis for the aim of studying the generation of ICP plateau waves in unstable conditions and sensitivity analysis for the aim of studying parameter sensitivity and estimation are other important goals defined for this study work.

Lack of mathematical model to describe the interrelationship between different aspects of intracranial dynamics and cerebral hemodynamics has recently become an important concern of some authors recently. Although some models have been suggested but the mathematical complexity and nonlinear relationships makes it almost impossible to be used in clinical approaches. Thus the need for a simple mathematical model to describe and investigate the biophysiology behind these interactions has become the center of attention for many researchers.

The analysis of ICP instability in this study suggests that high values of $K_E$ (poor intracranial compliance), $R_o$ (poor CSF absorption) and G ( poor/weak autoregulation) are the main reason favoring ICP instability and generation of self-sustained oscillations. Although the contained model contains several parameters but more detailed analysis in this study suggests that there are only few number of these parameters that play the pivotal role in influencing ICP time pattern including$K_E$, $R_o$, G and $\tau$. Thus one can estimate ICP time pattern by setting these parameters as priories and using an estimation algorithm for minimizing the cost function which is basically the difference between real data and simulated ICP.

The results obtained from this study are quite close to the ones suggested by Ursino both simple and complex model and can be also explained in terms of physiology of brain state [1, 32, 33, 48]. As shown in Figure 4.3 and 4.4 high values of $K_E$, $R_o$ and G are the main reasons for ICP instability and generation of self-sustained oscillations as shown in Figure 4.6. The bifurcation diagrams obtained from the stability analysis performed in this study suggests that there exists a

boundary at which ICP time pattern changes from stable to unstable form. This boundary is produced by the combination of the three mentioned parameters. In other words a high value of only one of these parameters is favorable but not enough for ICP to start oscillation, but both of parameters ($K_E$, $R_o$) or ($R_o$,G) should meet the boundary condition. More detailed explanation of mathematics supporting these results is presented in stability chapter. Moreover a preliminary sensitivity analysis performed in this study work proved that all parameters are not mainly influencing ICP but $K_E$, $R_o$ , G and $\tau$ show the most significant effect on ICP. Thus in ICP estimation/simulation procedure this set of parameters can be considered as priories and by setting other parameters to their nominal values a suitable minimization algorithm can estimate the value of these parameters in a way that the difference between clinical data and ICP becomes minimum (cost function minimization). Finally the correlation between parameters show how each two estimation parameters interact with each other. This might be useful for neuro-intensive care unit experts in decision making phase for choosing the right treatment that is beneficial for patient's status and has the minimum risk and danger.

Although this model is proved to be efficient in explaining most of the important features/ behaviors the same way that the complex model was used to, but there is always a price to be paid. In other words some limitations will arise in reproduction of physiological reality as a consequence of model's simplicity. One of the limitations introduced as a result of first simplification assumption implied to the complex model mentioned in the 'main simplification assumptions' section is the model's disability in distinguishing between the mechanisms working on large pial arteries and the ones working on small arterioles [1]. As mentioned before in the 'Qualitative description of the complex model' it has been insisted by several authors that large arteries are mostly controlled by pressure dependent mechanisms where small arterioles are controlled by flow dependent mechanisms.

The other shortcoming of this model is that it cannot be used in investigation of ICP pulsating wave containing cardiac and respiratory pulsations since it is highly affected by large intracranial arteries and venous circulation which are decided to be neglected in this model. Having said that, it is also worthy to mention that the model has the advantage of simplicity and physiological reliability over the complex model and can be directly used in neurosurgery intensive care units.

## 7.2 Future work

There are some interesting and useful studies that can be carried out later on for the aim of extending the level of our knowledge to a more detailed and informative one. Some suggestions for the further work could be the inclusion of other important mechanisms influencing intracranial dynamics such as respiratory and cardiac pulsation in analyzing pulsatile cerebral hemodynamics and inclusion of $CO_2$reactivity. The other possible suggestions could be a classification of patients according to their autoregulation level based on parameters optimal value gained by optimization algorithm.

## References

[1] Ursino, M., and C. A. Lodi. A simple mathematical model of the interaction between intracranial pressure and cerebral hemodynamics. Appl. Physiol. 82: 1256–1269, 1997.
[2] Penson R., Allen R. Intracranial hypertension: condition monitoring, simulation and time domain analysis. Eng. Sci. Educ. J. -- February 1999 -- Volume 8, Issue 1, p.33–40
[3] Avezaat, C. J. J., and J. H. M. van Eijndhoven. Cerebrospinal fluid pulse pressure and intracranial volume-pressure relationships.J. Neurol. Neurosurg. Psychiatry 42: 687–700, 1979.
[4] Charlton, J. D., H. A. Guess, J. D. Mann, H. T. Nagle, and R. N. Johnson. A pressure controller for estimating parameters for a nonlinear CSF model. IEEE Trans. Biomed. Eng. 35:752–754, 1988.
[5] Mann, J. D., A. B. Butler, J. E. Rosenthal, C. J. Maffeo, R. N. Johnson, and N. H. Bass. Regulation of intracranial pressure in rat, dog and man. Ann. Neurol. 3: 156–165, 1978.
[6] Czosnyka, M., N. G. Harris, J. D. Pickard, and S. Piechnik. CO2 cerebrovascular reactivity as a function of perfusion pressure— a modelling study. Acta Neurochir. 121: 159–165, 1993.
[7] Hoffman, H. Biomathematics of intracranial CSF and hemodynamics, simulation and analysis with the aid of a mathematical model. Acta Neurochir. Suppl. 40: 117–130, 1987.
[8] Sorek, S., J. Bear, and Z. Karni. Resistances and compliancesof a compartmental model of the cerebrovascular system. Ann. Biomed. Eng. 17: 1–12, 1989.
[9] Monro, A. Observations on the structure and function of the nervous system.Creech and Johnson, Edinburgh, 1783.
[10] Burrows, G. Disorders of the cerebral circulation system. Longman, London, 1846.
[11] Weed, L. H., and McKIBBEN, P. S. Experimental alteration of brain bulk. Am.J Physiol., 1919, 48, pp.531-558.
[12] Cushing, H. Some experimental and clinical observations concerning states of increased intracranial tension. Am. J. Med. Sci., 1902, 124, pp.375-400.
[13] Ayala, G. Die Physiopathologie der Mechanik des Liquor Cerebrospinalis und der Rachidealquotient. Mdu. Psychiat. Neurol., 1925, 58, pp.65-101.
[14] Weed, L. H., and Flexner, L. B. The relations of the intracranial pressures. Am. J Physiol., 1933, 105 pp.266-272.
[15] Cushing, H. Some experimental and clinical observations concerning states of increased intracranial tension. Am.J Med. Sci., 1902, 124, pp.375-400.
[16] Ryder, H. W et al. The elasticity of the craniospinal venous bed . Lab. Clin. Med., 1953, 42, p.944.
[17] Shulman, K., and Marmarou, A. Pressure volume considerations in infantile hydrocephalus. Dw. Med. Child Neurol., 1971, 13, suppl. 25, pp.9&95.
[18] Foltz, E. L., and Aine, B. S. Diagnosis of hydrocephalus by CSF pulse wave analysis. Sq. Neurol., April 1981, 15, (4), pp.283-293.

[19] Marmarou, A., K. Shulman, and J. LaMorgese. Compartmental analysis of compliance and outflow resistance of the cerebrospinal fluid system. J. Neurosurg. 43: 523–534, 1975.
[20] Risberg, J., N. Lundberg, and D. H. Ingvar**.** Regional cerebral blood volume during acute transient rises of the intracranial pressure (plateau waves). J. Neurosurg. 31: 303–310, 1969.
[21] Shahsasvari S. Intracranial pressure in traumatic brain injury, Chalmers University of Technology, Department of Signals and Systems, Göteborg, Sweden, No R006/2009.
[22] J. H. van Blankenstein, C. J. Slager, L. K. Soei, H. Boersma, and P. D. Verdouw. Effect of arterial blood pressure and ventilation gases on cardiac depression induced by coronary air embolism. J Appl Physiol, Oct 1994; 77: 1896 - 1902.
[23] Davson H. Formation and drainage of the CSF in hydrocephalus. New York: Raven Press. 1984. pp 112–60
[24] Czosnyka M., Czosnyka Z., Momjian S., and John D Pickard. Cerebrospinal fluid dynamics. Academic Neurosurgical Unit, Department of Neurosciences, Addenbrooke's Hospital,Cambridge, UK. 2004
[25] Davson H, Welch K and Segal M B. The Physiology and Pathophysiology of Cerebrospinal Fluid. 1987, New York, Churchill Livingstone.
[26] Aaslid, R., K. Lindegaard, W. Sorteberg, and H. Nornes**.** Cerebral autoregulation dynamics in humans. Stroke 20: 45–52, 1989.
[27] Ursino, M., M. Iezzi, and N. Stocchetti. Intracranial pressure dynamics in patients with acute brain damage: a critical analysis with the aid of a mathematical model. IEEE Trans. Biomed. Eng. 42: 529–540, 1995.
[28] Avezaat, C. J. J., and J. H. M. van Eijndhoven. The conflict between CSF pulse pressure and volume-pressure response during plateau waves. In: Intracranial Pressure V, edited by I.
Ishii, H. Nagai, and M. Brock. Berlin: Springer-Verlag, 1983, p. 326–332.
[29] Cold, G. E., and F. T. Jensen. Cerebral autoregulation in unconscious patients with brain injury. Acta Anaesthesiol. Scand. 22: 270–280, 1978.
[30] Paulson, O. B., S. Strandgaard, and L. Edvinsson. Cerebral autoregulation. Cerebrovasc. Brain Metab. Rev. 2: 161–192, 1990.
[31] Paulson OB and Waldemar G. Role of the local renin-angiotensin system in the autoregulation of the cerebral circulation. Blood Vessels 28: 231–235, 1991.
[32] Ursino, M., and P. Di Giammarco. A mathematical model of the relationship between cerebral blood volume and intracranial pressure changes: the generation of plateau waves. Ann. Biomed. Eng. 19: 15–42, 1991.
[33] Ursino, M. A mathematical study of human intracranial hydrodynamics. 1. The cerebrospinal fluid pulse pressure. Ann. Biomed. Eng. 16: 379–402, 1988.
[34] H. A. Kontos, E. P. Wei, R. M. Navari, J. E. Levasseur, W. I. Rosenblum, and J. L. Patterson, "Responses of cerebral arteries and arterioles to acute hypotension and hypertension," Amer. J. Physiol., vol. 234, pp. H371-H383, 1978.
[35] G. Mchedlishvili, Arterial Behavior and Blood Circulation in the Brain. New York: Plenum, 1986

[36] M. Kosteljanetz, "Intracranial pressure: Cerebrospinal fluid dynamics and pressure-volume relations," Acta Neurolog. Scand., suppl. 11 1, vol. 75, pp. 1-23, 1987.
[37] Avezaat, C. J. J., and J. H. M. van Eijndhoven. The role of the pulsatile pressure variations in intracranial pressure monitoring. Neurosurg. Rev. 9: 113–120, 1986.
[38] Marmarou, A., K. Shulman, and R. M. Rosende. A nonlinear analysis of the cerebrospinal fluid system and intracranial pressure dynamics. J. Neurosurg. 48: 332–344, 1978.
[39] Marmarou, A., R. L. Anderson, J. D. Ward, S. C. Choi, H. F. Young, H. M. Eisenberg, M. A. Foulkes, L. F. Marshall, and J. A. Jane. Impact of ICP instability and hypotension on outcome in patients with severe head trauma. J. Neurosurg. 75, Suppl.: 959–966, 1991.
[40] Shapiro K and Marmarou A. Abnormal brain compliance as a cause of hydrocephalus in children. In: Intracranial Pressure V. S Ishii, H Nagai and M Brock (eds). Springer-Verlag, Berlin, Heidelberg pp. 622-627, 1983.
[41] Rosner, M. J., and D. P. Becker. Origin and evolution of plateau waves. Experimental observation and a theoretical model. J. Neurosurg. 60: 312–324, 1984.
[42] Rosner, M. J., and S. Daughton. Cerebral perfusion pressure management in head injury. J. Trauma 30: 933–941, 1990.
[43] Rosner, M. J. Cerebral perfusion pressure: link between intracranial pressure and systemic circulation. In: Cerebral Blood Flow, edited by J. H. Wood. New York: McGraw-Hill, 1987, p. 425–448.
[44] Hassan K. Khalil. Nonlinear systems, second edition. Michigan State University, Prentice Hall, Upper Saddle River, NJ 07458.
[45] J. Guckenheimer and P. Holmes. Nonlinear Oscillations, Dynamical Systems, and Bifurcations of Vector Fields. Springer-Verlag, New York, 1983.
[46] J. Hale and H. Kocak. Dynamics and Bifurcations. Springer-Verlag, New York, 1991.
[47] L. Guzzella and **A.** H. Glattfelder. Stability of multivariable systems with saturating power amplifiers. In American Control Conference, pages 1687- 1692, June 1989.
[48] Ursino, M., C. A. Lodi, S. Rossi, and N. Stocchetti. Intracranial pressure dynamics in patients with acute brain damage. J. Appl. Physiol. 82: 1270–1282, 1997.
[49] Delwel, E. J., D. A. de Jong, and C. J. J.Avezaat. The relative prognostic value of CSF outflow resistance measurement in shunting for normal pressure hydrocephalus. In: Intracranial Pressure VIII, edited by C. J. J.Avezaat, J. H. M. van Eijndhoven, A. I. R. Maas, and J. T. J. Tans. Berlin: Springer-Verlag, 1993, p. 816–820.
[50] Eijndhoven, J. H. M. van, S. Sliwka, and C. J. J. Avezaat. The constant pressure term (P0) of the volume-pressure relationship. Comparison between results of infusion test and pulse pressure analysis. In: Intracranial Pressure VI, edited by J. D. Miller, G. M. Teasdale, J. O. Rowan, S. L. Galbraith, and A. D. Mendelow. Berlin: Springer-Verlag, 1986, p. 48–53.